Electromagnetic gauge field interpolation between the instant form and the front form of the Hamiltonian dynamics

Chueng-Ryong Ji,[1] Ziyue Li,[1] and Alfredo Takashi Suzuki[2]

[1]*Department of Physics, North Carolina State University, Raleigh, North Carolina 27695-8202, USA*
[2]*Instituto de Física Teórica-UNESP Universidade Estadual Paulista, Rua Doutor Bento Teobaldo Ferraz, 271—Bloco II—01140-070, São Paulo, São Paulo, Brazil*

(Received 16 November 2014; published 17 March 2015)

We present the electromagnetic gauge field interpolation between the instant form and the front form of the relativistic Hamiltonian dynamics and extend our interpolation of the scattering amplitude presented in the simple scalar field theory to the case of the electromagnetic gauge field theory with the scalar fermion fields known as the scalar quantum electrodynamics (sQED) theory. We find that the Coulomb gauge in the instant form dynamics and the light-front gauge in the front form dynamics, or the light-front dynamics (LFD), are naturally linked by the unified general physical gauge that interpolates between these two forms of dynamics and derive the spin-1 polarization vector for the photon that can be generally applicable for any interpolation angle. The corresponding photon propagator for an arbitrary interpolation angle is found and examined in terms of the gauge field polarization and the interpolating time ordering. Using these results, we calculate the lowest-order scattering processes for an arbitrary interpolation angle in sQED. We provide an example of breaking the reflection symmetry under the longitudinal boost, $P^z \leftrightarrow -P^z$, for the time-ordered scattering amplitude in any interpolating dynamics except the LFD and clarify the confusion in the prevailing notion of the equivalence between the infinite momentum frame and the LFD. The particular correlation found in our previous analysis of the scattering amplitude in the simple scalar field theory, coined as the J-shaped correlation, between the total momentum of the system and the interpolation angle persists in the present analysis of the sQED scattering amplitude. We discuss the singular behavior of this correlation in conjunction with the zero-mode issue in the LFD.

DOI: 10.1103/PhysRevD.91.065020 PACS numbers: 11.30.Cp, 11.55.Bq, 11.80.Cr

I. INTRODUCTION

In 1949, Dirac [1] proposed three forms of relativistic dynamics: the instant form ($x^0 = 0$), the front form ($x^+ = (x^0 + x^3)/\sqrt{2}$=0), and the point form ($x^\mu x_\mu = a^2 > 0, x^0 > 0$). While the quantization at the equal time $t = x^0$ produces the instant form dynamics (IFD) of quantum field theory, the quantization at equal light-front time $\tau \equiv (t + z/c)/\sqrt{2} = x^+$ (c is taken to be one unit in this work) yields the front form dynamics, known as the light-front dynamics (LFD). The quantization in the point form ($x^\mu x_\mu = a^2 > 0, x^0 > 0$) is called radial quantization, and this quantization procedure has been much used in string theory and conformal field theories [2]. Although the point form dynamics has also been explored [3] in hadron physics, the IFD and the LFD are still the most popular choices in the area of physics that we discuss here.

One of the reasons why the LFD is useful may be attributed to the energy-momentum dispersion relation. For a particle of mass m that has 4-momentum $k = (k^0, k^1, k^2, k^3)$, its energy-momentum dispersion relation at equal t (instant form) is given by

$$k^0 = \sqrt{\mathbf{k}^2 + m^2}, \tag{1}$$

where the energy k^0 is conjugate to t and the 3-momentum vector $\mathbf{k}$ is given by $\mathbf{k} = (k^1, k^2, k^3)$. On the other hand, the corresponding energy-momentum relation at equal τ (light-front form) is given by

$$k^- = \frac{\mathbf{k}_\perp^2 + m^2}{k^+}, \tag{2}$$

where the light-front energy $k^- = (k^0 - k^3)/\sqrt{2}$ is conjugate to τ and the light-front momenta $k^+ = (k^0 + k^3)/\sqrt{2}$ and $\mathbf{k}_\perp = (k^1, k^2)$ are orthogonal to k^-. In contrast to the irrational dispersion relation Eq. (1) in the IFD, this rational energy-momentum relation Eq. (2) in the LFD not only makes the relation simpler but also correlates the sign of k^- and k^+. When the system is evolving to the future direction (i.e., positive τ), in order for k^- to be positive, k^+ also has to be positive. This feature prevents certain processes from happening in the LFD; for example, the spontaneous pair production from the vacuum is forbidden unless $k^+ = 0$ for both particles due to the momentum conservation. Some dynamic processes are therefore eliminated in the LFD, and correspondingly the required computation may be simplified, although we shall discuss the zero-mode issue involving the case of $k^+ = 0$ later. In the IFD, however, this type of sign correlation does not exist, and the vacuum structure appears much more

 © 2015 American Physical Society

complicated than in the case of LFD due to the quantum fluctuations. This difference in the energy-momentum dispersion relation makes the LFD quite distinct from other forms of the relativistic Hamiltonian dynamics.

Furthermore, the Poincaré algebra is drastically changed in the LFD compared to the IFD. In the LFD, we have the maximum number (seven) of kinematic (i.e., interaction independent) operators out of the ten Poincaré generators, and they leave the state at $\tau = 0$ unchanged. In particular, the longitudinal boost operator joins the stability group of kinematic operators in the LFD. This built-in boost invariance together with the simpler vacuum property makes the LFD quite appealing and may save substantial computational efforts to get the QCD solutions that reflect the full Poincaré symmetries.

The light-front quantization [1,4] has been applied successfully in the context of current algebra [5] and the parton model [6] in the past. With further advances in the Hamiltonian renormalization program [7,8], the LFD appears to be even more promising for the relativistic treatment of hadrons. In the work of Brodsky *et al.* [9], it is demonstrated how to solve the problem of renormalizing light-front Hamiltonian theories while maintaining Lorentz symmetry and other symmetries. The genesis of the work presented in Ref. [9] may be found in Ref. [10], and additional examples including the use of LFD methods to solve the bound-state problems in field theory can be found in the review of QCD and other field theories on the light front [11]. A possible realization of chiral symmetry breaking in the light-front vacuum has also been discussed in the literature [12].

However, the transverse rotation of which the direction is perpendicular to the direction of the quantization axis z at equal τ becomes a dynamical problem in the LFD because the quantization surface τ is not invariant under the transverse rotation and the transverse angular momentum operator involves the interaction that changes the particle number [13].

As an effort to understand the conversion of the dynamical problem from boost to rotation as well as the link between the IFD and the LFD, we interpolate the two forms of dynamics by introducing an interpolation angle that changes the ordinary time t to the light-front time τ or vice versa. The same method of interpolating hypersurfaces has been used by Hornbostel [14] to analyze various aspects of field theories including the issue of nontrivial vacuum. The same vein of application to study the axial anomaly in the Schwinger model has also been presented [15], and other related works [16–19] can also be found in the literature.

Our interpolation between the IFD and the LFD provides the whole picture of landscape between the two and clarifies the issue, if any, in linking them to each other. We started out by studying the Poincaré algebra for any arbitrary interpolation angle [20] and provided the physical meaning of the kinematic vs dynamic operators by introducing the interpolating time-ordered scattering amplitudes [21]. Although we want ultimately to obtain a general formulation for the QED and the QCD using the interpolation between the IFD and the LFD, we start from the simpler theory to discuss first the bare-bone structure that will persist even in the more complicated theories. Since we have studied the simple scalar field theory [21] involving just the fundamental degrees of freedom such as the momenta of particles in scattering processes, we now consider involving the electromagnetic gauge degree of freedom interpolated between the IFD and the LFD in the present work. We develop the electromagnetic gauge field propagator interpolated between the IFD and the LFD and extend our interpolation of the scattering amplitude presented in the simple scalar field theory to the case of the electromagnetic gauge field theory but still with the scalar fermion fields known as the sQED theory.

In LFD, the light-front gauge $[A^+ = (A^0 + A^3)/\sqrt{2} = 0]$ is commonly used, since the transverse polarizations of the gauge field can be immediately identified as the dynamical degrees of freedom, and ghost fields can be ignored in the quantum action of non-Abelian gauge theory [22–24]. This makes it especially attractive in various QCD applications. We find that the light-front gauge in the LFD is naturally linked to the Coulomb gauge in the IFD through the interpolation angle. The corresponding gauge propagator that interpolates between the IFD and the LFD also sheds light on the debate about whether the gauge propagator should be the two-term form [8] or the three-term form [25–27]. For example, by analyzing the lowest-order sQED Feynman amplitude, one may typically get the corresponding three time-ordered amplitudes, one of which corresponds to the contribution from the instantaneous interaction of the gauge field. This contribution from the instantaneous interaction is, however, precisely canceled by one of the terms in the three-term gauge propagator, and thus the two-term gauge propagator may also be used effectively for the calculation of the same Feynman amplitude without involving the instantaneous interaction of the gauge field. Otherwise, to maintain the equivalence to the covariant formulation, the three-term propagator should be used including the instantaneous interaction of the gauge field.

Our work also clarifies the singular nature of the correlation between the total momentum of the system and the interpolation angle and provides a deeper understanding of the treacherous zero-mode issue in the LFD. We find that the particular correlation between the total momentum of the system and the interpolation angle, coined as the J-shaped correlation in our previous analysis, persists even in the sQED scattering amplitude involving the gauge field. We discuss the universal nature of the J-shaped correlation that appears completely independent from the nature of particles (i.e., mass, spin, etc.) involved in the scattering process.

Although the interpolation method has been introduced before [14,15,20,21], it has not yet been widely explored, and a brief description of the method is still necessary for the presentation of our work. In Sec. II, we thus provide a brief review of the interpolation angle method essential for the rest of this article. In Sec. III, we derive the photon polarization vector for any interpolation angle. Using this derivation, we present the general gauge that links the light-front gauge to the Coulomb gauge and construct the corresponding photon propagator for an arbitrary interpolation angle. In Sec. IV, we decompose this interpolating gauge propagator according to the time ordering and apply it to the lowest scattering process such as an analog of the well-known QED process $e\mu \to e\mu$ in sQED without involving the fermion spins. We also take a close look at the limiting cases of $\mathbb{C} \to 0$ and compare the results with the exact $\mathbb{C} = 0$ (LFD) results in this section. In Sec. V, we plot the time-ordered amplitudes in terms of the total momentum of the system and the interpolation angle to reveal both the frame dependence and interpolation angle dependence of these amplitudes. We then give a detailed discussion of the universal J-shaped correlation curve that emerges from these time-ordered diagrams and how it gives rise to the zero-mode contributions at $P^z = -\infty$. A summary and conclusion follow in Sec. VI.

In Appendix A, we list the explicit matrix representation of the boost $\mathbf{K}$ and rotation $\mathbf{J}$ generators and provide the explicit description of the steps involved in deriving the photon polarization vectors for an arbitrary interpolation angle. In Appendix B, we derive the numerator of the photon propagator from the photon polarization vectors for an arbitrary interpolation angle. In Appendix C, we decompose the photon propagator on the light front in terms of the transverse and longitudinal components. For the completeness and the comparison with our analysis of sQED scattering process (analogous to $e\mu \to e\mu$ in QED) presented in Secs. IV and V, we present in Appendixes D and E our calculations for the same process "$e\mu \to e\mu$" in the scalar field theory and the process related by the crossing symmetry "$e^+e^- \to \mu^+\mu^-$" in sQED. Together with our previous work for the scalar field theory discussed in Ref. [21], this work completes our study of the lowest-order scattering processes related by the crossing symmetry in the scalar field theory as well as in sQED.

II. METHOD OF INTERPOLATION ANGLE

In this section, we briefly review the interpolation angle method, presenting just the necessary formulas for the present work. For more detailed introduction and review of this method, the readers may consult our previous works presented in Refs. [20] and [21].

The interpolating space-time coordinates may be defined as a transformation from the ordinary space-time coordinates, $x^{\hat{\mu}} = \mathcal{R}^{\hat{\mu}}{}_{\nu} x^{\nu}$, i.e.,

$$\begin{pmatrix} x^{\hat{+}} \\ x^{\hat{1}} \\ x^{\hat{2}} \\ x^{\hat{-}} \end{pmatrix} = \begin{pmatrix} \cos\delta & 0 & 0 & \sin\delta \\ 0 & 1 & 0 & 0 \\ 0 & 0 & 1 & 0 \\ \sin\delta & 0 & 0 & -\cos\delta \end{pmatrix} \begin{pmatrix} x^0 \\ x^1 \\ x^2 \\ x^3 \end{pmatrix}, \quad (3)$$

where $0 \le \delta \le \pi/4$ is the interpolation angle. Following Ref. [21], we use "$\hat{}$" on the indices to denote the interpolating variables with the parameter δ. In the limits $\delta \to 0$ and $\delta \to \pi/4$, we recover the corresponding variables in the instant form and the front form, respectively. For example, the interpolating coordinates $x^{\hat{\pm}}$ in the limit $\delta \to \pi/4$ become the light-front coordinates $x^{\pm} = (x^0 \pm x^3)/\sqrt{2}$ without $\hat{}$.

In this interpolating basis, the metric becomes

$$g^{\hat{\mu}\hat{\nu}} = g_{\hat{\mu}\hat{\nu}} = \begin{pmatrix} \mathbb{C} & 0 & 0 & \mathbb{S} \\ 0 & -1 & 0 & 0 \\ 0 & 0 & -1 & 0 \\ \mathbb{S} & 0 & 0 & -\mathbb{C} \end{pmatrix}, \quad (4)$$

where $\mathbb{S} = \sin 2\delta$ and $\mathbb{C} = \cos 2\delta$. The covariant interpolating space-time coordinates are then easily obtained as

$$x_{\hat{\mu}} = g_{\hat{\mu}\hat{\nu}} x^{\hat{\nu}} = \begin{pmatrix} x_{\hat{+}} \\ x_{\hat{1}} \\ x_{\hat{2}} \\ x_{\hat{-}} \end{pmatrix} = \begin{pmatrix} \cos\delta & 0 & 0 & -\sin\delta \\ 0 & -1 & 0 & 0 \\ 0 & 0 & -1 & 0 \\ \sin\delta & 0 & 0 & \cos\delta \end{pmatrix} \times \begin{pmatrix} x^0 \\ x^1 \\ x^2 \\ x^3 \end{pmatrix}. \quad (5)$$

The same transformations also apply to the momentum:

$$P^{\hat{+}} = P^0 \cos\delta + P^3 \sin\delta, \quad (6a)$$

$$P^{\hat{-}} = P^0 \sin\delta - P^3 \cos\delta, \quad (6b)$$

$$P_{\hat{+}} = P^0 \cos\delta - P^3 \sin\delta, \quad (6c)$$

$$P_{\hat{-}} = P^0 \sin\delta + P^3 \cos\delta. \quad (6d)$$

Since the perpendicular components remain the same ($a^{\hat{j}} = a^j, a_{\hat{j}} = a_j, j = 1, 2$), we will omit the $\hat{}$ notation unless necessary from now on for the perpendicular indices $j = 1, 2$ in a 4-vector.

Using $g^{\hat{\mu}\hat{\nu}}$ and $g_{\hat{\mu}\hat{\nu}}$, we see that the covariant and contravariant components are related by

$$a_{\hat{+}} = \mathbb{C}a^{\hat{+}} + \mathbb{S}a^{\hat{-}}; \qquad a^{\hat{+}} = \mathbb{C}a_{\hat{+}} + \mathbb{S}a_{\hat{-}}$$
$$a_{\hat{-}} = \mathbb{S}a^{\hat{+}} - \mathbb{C}a^{\hat{-}}; \qquad a^{\hat{-}} = \mathbb{S}a_{\hat{+}} - \mathbb{C}a_{\hat{-}}$$
$$a_j = -a^j, \qquad (j = 1, 2). \tag{7}$$

The inner product of two 4-vectors must be interpolation angle independent as one can verify

$$a^{\hat{\mu}}b_{\hat{\mu}} = (a_{\hat{+}}b_{\hat{+}} - a_{\hat{-}}b_{\hat{-}})\mathbb{C} + (a_{\hat{+}}b_{\hat{-}} + a_{\hat{-}}b_{\hat{+}})\mathbb{S} - a_1b_1 - a_2b_2 = a^{\mu}b_{\mu}. \tag{8}$$

In particular, we have the energy-momentum dispersion relation given by

$$P^{\hat{\mu}}P_{\hat{\mu}} = P^2_{\hat{+}}\mathbb{C} - P^2_{\hat{-}}\mathbb{C} + 2P_{\hat{+}}P_{\hat{-}}\mathbb{S} - \mathbf{P}^2_{\perp}. \tag{9}$$

Another useful relation,

$$P^{\hat{\mu}}P_{\hat{\mu}}\mathbb{C} = P^{\hat{+}2} - P^2_{\hat{-}} - \mathbf{P}^2_{\perp}\mathbb{C}, \tag{10}$$

can also be easily verified. For the particles of mass M, $P^{\mu}P_{\mu}$ on the mass shell equals M^2, of course.

Accordingly, the Poincaré matrix

$$M^{\mu\nu} = \begin{pmatrix} 0 & K^1 & K^2 & K^3 \\ -K^1 & 0 & J^3 & -J^2 \\ -K^2 & -J^3 & 0 & J^1 \\ -K^3 & J^2 & -J^1 & 0 \end{pmatrix} \tag{11}$$

transforms as well, so

$$M^{\hat{\mu}\hat{\nu}} = \mathcal{R}^{\hat{\mu}}_{\alpha}M^{\alpha\beta}\mathcal{R}^{\hat{\nu}}_{\beta} = \begin{pmatrix} 0 & E^{\hat{1}} & E^{\hat{2}} & -K^3 \\ -E^{\hat{1}} & 0 & J^3 & -F^{\hat{1}} \\ -E^{\hat{2}} & -J^3 & 0 & -F^{\hat{2}} \\ K^3 & F^{\hat{1}} & F^{\hat{2}} & 0 \end{pmatrix} \tag{12}$$

and

$$M_{\hat{\mu}\hat{\nu}} = g_{\hat{\mu}\hat{\alpha}}M^{\hat{\alpha}\hat{\beta}}g_{\hat{\beta}\hat{\nu}} = \begin{pmatrix} 0 & \mathcal{D}^{\hat{1}} & \mathcal{D}^{\hat{2}} & K^3 \\ -\mathcal{D}^{\hat{1}} & 0 & J^3 & -\mathcal{K}^{\hat{1}} \\ -\mathcal{D}^{\hat{2}} & -J^3 & 0 & -\mathcal{K}^{\hat{2}} \\ -K^3 & \mathcal{K}^{\hat{1}} & \mathcal{K}^{\hat{2}} & 0 \end{pmatrix}, \tag{13}$$

where

$$E^{\hat{1}} = J^2\sin\delta + K^1\cos\delta, \qquad \mathcal{K}^{\hat{1}} = -K^1\sin\delta - J^2\cos\delta,$$
$$E^{\hat{2}} = K^2\cos\delta - J^1\sin\delta, \qquad \mathcal{K}^{\hat{2}} = J^1\cos\delta - K^2\sin\delta,$$
$$F^{\hat{1}} = K^1\sin\delta - J^2\cos\delta, \qquad \mathcal{D}^{\hat{1}} = -K^1\cos\delta + J^2\sin\delta,$$
$$F^{\hat{2}} = K^2\sin\delta + J^1\cos\delta, \qquad \mathcal{D}^{\hat{2}} = -J^1\sin\delta - K^2\cos\delta. \tag{14}$$

The interpolating $E^{\hat{j}}$ and $F^{\hat{j}}$ will coincide with the usual E^j and F^j of the LFD in the limit $\delta = \pi/4$. Note here that the $\hat{}$ notation is reinstated for 1,2 to emphasize the angle δ dependence and that the position of the indices on $K, J, E, F, \mathcal{D}$, and $\mathcal{K}$ will not matter as they are not the 4-vectors: i.e., $E_{\hat{1}} = E^{\hat{1}}$, etc. Of course, $M^{\hat{\mu}\hat{\nu}}$ and $M_{\hat{\mu}\hat{\nu}}$ should be distinguished in any case.

The generalized Poincaré algebra for any interpolation angle can be found in Ref. [20]. Among the ten Poincaré generators, the six generators ($\mathcal{K}^{\hat{1}}, \mathcal{K}^{\hat{2}}, J^3, P_1, P_2$, and $P_{\hat{-}}$) are always kinematic in the sense that the $x^{\hat{+}} = 0$ plane is intact under the transformations generated by them. As discussed in Refs. [20,21], the operator $K^3 = M_{\hat{+}\hat{-}}$ is dynamical in the region where $0 \le \delta < \pi/4$ but becomes kinematic in the light-front limit ($\delta = \pi/4$). The set of kinematic and dynamic generators depending on the interpolation angle are summarized in Table I. Since the kinematic transformations do not alter $x^{\hat{+}}$, the individual time-ordered amplitude must be invariant under the kinematic transformations. This can be seen explicitly in the example of scattering process discussed in Secs. IV and V.

Using the kinematic transformations defined above and following the procedure presented by Jacob and Wick [28] to define the helicity in the IFD, we may define the helicity applicable to any arbitrary interpolation angle δ. For this purpose, we introduced the transformation T [20,21] given by

$$T = T_{12}T_3 = e^{i\beta_1\mathcal{K}^{\hat{1}} + i\beta_2\mathcal{K}^{\hat{2}}}e^{-i\beta_3K^3}, \tag{15}$$

where we consider the operation on the state such as $T_{12}T_3|\psi\rangle$ in this work rather than the operation on the operator as discussed in our previous work [20,21]. As shown in the textbook example of the body-fixed frame vs the space-fixed frame in the Euler angle rotation in the

TABLE I. Kinematic and dynamic generators for different interpolation angles.

	Kinematic	Dynamic
$\delta = 0$	$\mathcal{K}^{\hat{1}} = -J^2, \mathcal{K}^{\hat{2}} = J^1, J^3, P^1, P^2, P^3$	$\mathcal{D}^{\hat{1}} = -K^1, \mathcal{D}^{\hat{2}} = -K^2, K^3, P^0$
$0 \le \delta < \pi/4$	$\mathcal{K}^{\hat{1}}, \mathcal{K}^{\hat{2}}, J^3, P^1, P^2, P_{\hat{-}}$	$\mathcal{D}^{\hat{1}}, \mathcal{D}^{\hat{2}}, K^3, P_{\hat{+}}$
$\delta = \pi/4$	$\mathcal{K}^{\hat{1}} = -E^1, \mathcal{K}^{\hat{2}} = -E^2, J^3, K^3, P^1, P^2, P^+$	$\mathcal{D}^{\hat{1}} = -F^1, \mathcal{D}^{\hat{2}} = -F^2, P^-$

rigid-body problem, the order of operation on the operator can be reversed in constructing the Euler angle rotation depending on the choice of frame in the operation [29]. The similar type of reverse in the order of operation can occur in the case that the operation of T is applied to the operator rather than to the state. Thus, one should be careful when applying the operation of T to the operator rather than to the state, as we have discussed in our previous work [21]. In this work, we simplify the discussion by considering the operation of T to the state instead of the operator. We also adopt the sign convention of the exponents $i\beta_1\mathcal{K}^{\hat{1}}$ and $i\beta_2\mathcal{K}^{\hat{2}}$ of T_{12} to make the resulted momentum positive for the infinitesimal positive values of β_1 and β_2. Our sign convention in this work turns out to be consistent with Soper's notation [30] in the LFD.

Using the transformation given by Eq. (15), we obtain the 4-momentum components ($P'^{\hat{+}}, P'^1, P'^2$, and $P'_{\hat{-}}$) from the initial 4-momentum components ($P^{\hat{+}}, P^1, P^2$, and $P_{\hat{-}}$) [20,21],

$$P'^{\hat{+}} = P^{\hat{+}}\cosh\beta_3 + P_{\hat{-}}\sinh\beta_3, \tag{16a}$$

$$P'^1 = P^1 + \beta_1\frac{\sin\alpha}{\alpha}(P_{\hat{-}}\cosh\beta_3 + P^{\hat{+}}\sinh\beta_3) + \frac{\cos\alpha - 1}{\alpha^2}\mathbb{C}\beta_1(\beta_1 P^1 + \beta_2 P^2), \tag{16b}$$

$$P'^2 = P^2 + \beta_2\frac{\sin\alpha}{\alpha}(P_{\hat{-}}\cosh\beta_3 + P^{\hat{+}}\sinh\beta_3) + \frac{\cos\alpha - 1}{\alpha^2}\mathbb{C}\beta_2(\beta_1 P^1 + \beta_2 P^2), \tag{16c}$$

$$P'_{\hat{-}} = (P_{\hat{-}}\cosh\beta_3 + P^{\hat{+}}\sinh\beta_3)\cos\alpha + \frac{\sin\alpha}{\alpha}\mathbb{C}(\beta_1 P^1 + \beta_2 P^2), \tag{16d}$$

where $\alpha = \sqrt{\mathbb{C}(\beta_1^2 + \beta_2^2)}$. Although these 4-momentum components ($P'^{\hat{+}}, P'^1, P'^2$, and $P'_{\hat{-}}$) given by Eqs. (16a)–(16d) turn out to be most convenient in carrying out our calculation, the other choice of components such as $P'_{\hat{+}}$ and $P'^{\hat{-}}$ can be easily obtained using Eq. (7).

As an example of using Eqs. (16a)–(16d), we may find that the particle of mass M at rest gains the 4-momentum components under the transformation T,

$$P^{\hat{+}} = (\cos\delta\cosh\beta_3 + \sin\delta\sinh\beta_3)M, \tag{17a}$$

$$P^1 = \beta_1\frac{\sin\alpha}{\alpha}(\sin\delta\cosh\beta_3 + \cos\delta\sinh\beta_3)M, \tag{17b}$$

$$P^2 = \beta_2\frac{\sin\alpha}{\alpha}(\sin\delta\cosh\beta_3 + \cos\delta\sinh\beta_3)M, \tag{17c}$$

$$P_{\hat{-}} = \cos\alpha(\sin\delta\cosh\beta_3 + \cos\delta\sinh\beta_3)M, \tag{17d}$$

where the factor $(\sin\delta\cosh\beta_3 + \cos\delta\sinh\beta_3)$ in the 3-momentum $(P^1, P^2, P_{\hat{-}})$ is due to the first boost $T_3 = e^{-i\beta_3\mathcal{K}^3}$. Our convention of taking this factor to be positive, i.e., $(\sin\delta\cosh\beta_3 + \cos\delta\sinh\beta_3) > 0$, is consistent with the convention taken by Jacob and Wick [28] in their procedure to define the helicity in the IFD. We also note that $P_{\hat{-}} = M\sin\delta$, $P^{\hat{+}} = M\cos\delta$, and $P^1 = P^2 = 0$ in the particle rest frame.

Solving Eqs. (17a)–(17d) for β_1, β_2, and β_3, we further note that

$$\sin\delta\cosh\beta_3 + \cos\delta\sinh\beta_3 = \frac{\mathbb{P}}{M}, \tag{18a}$$

$$\cos\delta\cosh\beta_3 + \sin\delta\sinh\beta_3 = \frac{P^{\hat{+}}}{M}, \tag{18b}$$

and

$$\cos\alpha = \frac{P_{\hat{-}}}{\mathbb{P}}, \tag{19a}$$

$$\sin\alpha = \frac{\sqrt{\mathbf{P}_\perp^2\mathbb{C}}}{\mathbb{P}}, \tag{19b}$$

$$e^{\beta_3} = \frac{P^{\hat{+}} + \mathbb{P}}{M(\sin\delta + \cos\delta)}, \tag{19c}$$

$$e^{-\beta_3} = \frac{P^{\hat{+}} - \mathbb{P}}{M(\cos\delta - \sin\delta)}, \tag{19d}$$

$$\frac{\beta_j}{\alpha} = \frac{P^j}{\sqrt{\mathbf{P}_\perp^2\mathbb{C}}}, \qquad (j = 1, 2), \tag{19e}$$

where $\mathbb{P} \equiv \sqrt{P_{\hat{-}}^2 + \mathbf{P}_\perp^2\mathbb{C}}$ corresponds to the magnitude of the particle's 3-momentum in the IFD, while it becomes identical to P^+ in the limit $\delta \to \pi/4$ so that $\alpha = 0$, i.e., $\cos\alpha = 1$ and $\sin\alpha = 0$, in the LFD, as one can see from Eqs. (19a) and (19b), respectively. Multiplying Eqs. (19c) and (19d), we get the on-mass-shell condition consistent with Eq. (10) for the particle of rest mass M:

$$P_{\hat{-}}^2 + \mathbf{P}_\perp^2\mathbb{C} = (P^{\hat{+}})^2 - M^2\mathbb{C}. \tag{20}$$

Consequently, the quantity denoted by $\mathbb{P} = \sqrt{P_{\hat{-}}^2 + \mathbf{P}_\perp^2\mathbb{C}}$ can also be written as $\mathbb{P} = \sqrt{(P^{\hat{+}})^2 - M^2\mathbb{C}}$. We note again the correspondence of $\mathbb{P}$ to $\sqrt{(P^3)^2 + \mathbf{P}_\perp^2} = |\mathbf{P}|$ in the limit $\delta \to 0$ (or $\mathbb{C} \to 1$) and $\mathbb{P}$ to P^+ in the limit $\delta \to \pi/4$ (or $\mathbb{C} \to 0$).

III. LINK BETWEEN THE COULOMB GAUGE AND THE LIGHT-FRONT GAUGE

We now discuss the gauge field in an arbitrary interpolation angle. Rather than fixing the gauge first, we start from the explicit physical polarization 4-vectors of the spin-1 particle and then identify the corresponding gauge that these explicit representations of the gauge field polarization satisfy. This procedure is possible because we can follow the Jacob–Wick procedure discussed in Sec. II and apply the corresponding T transformation [Eq. (15)] to the rest frame spin-1 particle polarization vectors that may be naturally given by the spherical harmonics. Although this procedure applies to the physical spin-1 particle with a nonzero mass M such as the ρ meson, we may take advantage of the Lorentz invariance of the 4-momentum squared $P^{\hat{\mu}}P_{\hat{\mu}} = M^2$ and replace M^2 by $P^{\hat{\mu}}P_{\hat{\mu}}$ to extend the obtained polarization 4-vectors to the virtual gauge particle. For the real photon, of course, $M = 0$, and the longitudinal polarization vector should be discarded. From this procedure, we find that the identified gauge interpolates between the Coulomb gauge in the instant form and the light-front gauge in the front form.

A. Spin-1 polarization vector for any interpolation angle

We use the 4-vector representation of Lorentz group for the spin-1 particle. The polarization vector in a specific frame is obtained by boosting the 4-vectors to that frame. In the rest frame, where the 4-momentum is $(M, 0, 0, 0)$, the polarization vectors are taken to be

$$\epsilon(\pm) = \mp\frac{1}{\sqrt{2}}(0, 1, \pm i, 0), \qquad \epsilon(0) = (0, 0, 0, 1), \tag{21}$$

since the spherical harmonics $Y_1^{\pm 1}$ and Y_1^0 naturally correspond to the transverse and longitudinal polarization vectors, respectively.

To find the polarization vectors of the spin-1 particle with an arbitrary momentum $P^{\hat{\mu}}$, we use the Jacob–Wick procedure discussed in Sec. II and apply the T transformation [Eq. (15)] with the explicit 4-vector representation of the operators $\mathbf{K}$ and $\mathbf{J}$. The details of the calculation are summarized in Appendix A. The result of the polarization vectors written in the form of $(\epsilon_{\hat{+}}, \epsilon_1, \epsilon_2, \epsilon_{\hat{-}})$ is given by

$$\epsilon_{\hat{\mu}}(P, +) = -\frac{1}{\sqrt{2}\mathbb{P}}\left(\mathbb{S}|\mathbf{P}_\perp|, \frac{P_1P_{\hat{-}} - iP_2\mathbb{P}}{|\mathbf{P}_\perp|}, \frac{P_2P_{\hat{-}} + iP_1\mathbb{P}}{|\mathbf{P}_\perp|}, -\mathbb{C}|\mathbf{P}_\perp|\right), \tag{22a}$$

$$\epsilon_{\hat{\mu}}(P, -) = \frac{1}{\sqrt{2}\mathbb{P}}\left(\mathbb{S}|\mathbf{P}_\perp|, \frac{P_1P_{\hat{-}} + iP_2\mathbb{P}}{|\mathbf{P}_\perp|}, \frac{P_2P_{\hat{-}} - iP_1\mathbb{P}}{|\mathbf{P}_\perp|}, -\mathbb{C}|\mathbf{P}_\perp|\right), \tag{22b}$$

$$\epsilon_{\hat{\mu}}(P, 0) = \frac{P^{\hat{+}}}{M\mathbb{P}}\left(P_{\hat{+}} - \frac{M^2}{P^{\hat{+}}}, P_1, P_2, P_{\hat{-}}\right). \tag{22c}$$

They satisfy the transversality and orthorgonality constraints

$$\epsilon_{\hat{\mu}}(P, \lambda)P^{\hat{\mu}} = 0, \qquad \epsilon^*(P, \lambda)\cdot\epsilon(P, \lambda') = -\delta_{\lambda\lambda'}. \tag{23}$$

It is also obvious that $\epsilon(P, 0)$ is "parallel" to the 3-momentum $\mathbf{P}$, since $(\epsilon_1, \epsilon_2, \epsilon_{\hat{-}}) \sim (P_1, P_2, P_{\hat{-}})$. Noticing that $\mathbb{S} \to 0$, $\mathbb{C} \to 1$, $\mathbb{P} \to |\mathbf{P}|$ when $\delta \to 0$ and $\mathbb{S} \to 1$, $\mathbb{C} \to 0$, $\mathbb{P} \to P^+$ when $\delta \to \pi/4$, one can easily check that these polarization vectors have correct limits of the instant form and the light-front form at $\delta = 0$ and $\delta = \pi/4$, respectively.

B. Interpolating transverse gauge

Having obtained the explicit polarization 4-vectors of the spin-1 particle with mass M, we notice that the transverse polarizations given by Eqs. (22a) and (22b) are independent of the particle mass M. Thus, they can be used also as the transverse polarization 4-vectors of the gauge field such as the photon.

We observe that the transverse polarization vectors ($\lambda = \pm$) in Eqs. (22a) and (22b) satisfy the conditions

$$\epsilon^{\hat{+}}(\lambda) = \mathbb{C}\epsilon_{\hat{+}}(\lambda) + \mathbb{S}\epsilon_{\hat{-}}(\lambda) = 0, \tag{24}$$

$$\epsilon_{\hat{-}}(\lambda)P_{\hat{-}} + \boldsymbol{\epsilon}_\perp(\lambda)\mathbf{P}_\perp\mathbb{C} = 0, \tag{25}$$

where we used $\epsilon_{\hat{\mu}}(\lambda) = \epsilon_{\hat{\mu}}(P, \lambda)$ for convenience. So, we can write the gauge condition for transverse photons as

$$A^{\hat{+}} = 0, \tag{26}$$

$$A_{\hat{-}}P_{\hat{-}} + \mathbf{A}_\perp\mathbf{P}_\perp\mathbb{C} = 0, \tag{27}$$

where the second condition can also be written as

$$\partial_{\hat{-}}A_{\hat{-}} + \boldsymbol{\partial}_\perp\mathbf{A}_\perp\mathbb{C} = 0. \tag{28}$$

We now demonstrate that these two conditions are closely related to each other. First of all, the Lorentz

condition $\partial_{\hat{\mu}}A^{\hat{\mu}} = 0$ is always satisfied, as already verified in Eq. (23). But the Lorentz condition can be rewritten as

$$\begin{aligned}
0 &= \partial_{\hat{\mu}}A^{\hat{\mu}} \\
&= \partial_{\hat{+}}A_{\hat{+}}\mathbb{C} - \partial_{\hat{-}}A_{\hat{-}}\mathbb{C} + \partial_{\hat{+}}A_{\hat{-}}\mathbb{S} + \partial_{\hat{-}}A_{\hat{+}}\mathbb{S} - \boldsymbol{\partial}_\perp\mathbf{A}_\perp \\
&= \partial_{\hat{+}}A^{\hat{+}} - \partial_{\hat{-}}A_{\hat{-}}\mathbb{C} + \partial_{\hat{-}}A_{\hat{+}}\mathbb{S} - \boldsymbol{\partial}_\perp\mathbf{A}_\perp \\
&= \partial_{\hat{+}}A^{\hat{+}} - \left(\frac{1-\mathbb{S}^2}{\mathbb{C}}\right)\partial_{\hat{-}}A_{\hat{-}} + \partial_{\hat{-}}A_{\hat{+}}\mathbb{S} - \boldsymbol{\partial}_\perp\mathbf{A}_\perp \\
&= \partial_{\hat{+}}A^{\hat{+}} + \frac{\mathbb{S}}{\mathbb{C}}(\mathbb{S}\partial_{\hat{-}}A_{\hat{-}} + \mathbb{C}\partial_{\hat{-}}A_{\hat{+}}) - \left(\frac{\partial_{\hat{-}}A_{\hat{-}}}{\mathbb{C}} + \boldsymbol{\partial}_\perp\mathbf{A}_\perp\right) \\
&= \frac{\mathbb{C}}{\mathbb{C}}\partial_{\hat{+}}A^{\hat{+}} + \frac{\mathbb{S}}{\mathbb{C}}(\partial_{\hat{-}}A^{\hat{+}}) - \left(\frac{\partial_{\hat{-}}A_{\hat{-}}}{\mathbb{C}} + \boldsymbol{\partial}_\perp\mathbf{A}_\perp\right) \\
&= \frac{1}{\mathbb{C}}\partial^{\hat{+}}A^{\hat{+}} - \left(\frac{\partial_{\hat{-}}A_{\hat{-}}}{\mathbb{C}} + \boldsymbol{\partial}_\perp\mathbf{A}_\perp\right) \\
&= \frac{1}{\mathbb{C}}[\partial^{\hat{+}}A^{\hat{+}} - (\partial_{\hat{-}}A_{\hat{-}} + \boldsymbol{\partial}_\perp\mathbf{A}_\perp\mathbb{C})],
\end{aligned} \tag{29}$$

where Eq. (8) is used in the second line and the relations in Eq. (7) are used to go between the superscript components and the subscript components. Equation (29) indicates that if Eq. (26) holds then we have Eq. (28). On the other hand, if Eq. (28) holds, then we have

$$\partial^{\hat{+}}A^{\hat{+}} = 0. \tag{30}$$

However, this is a differential equation, and we have the freedom to specify the boundary condition. And we can choose our boundary condition to make $A^{\hat{+}} = 0$. This same trick was used in the instant form [31] where the Coulomb gauge $\nabla\cdot\mathbf{A} = 0$ gives $\partial_0 A^0 = 0$, but we can choose our initial condition, or gauge, so that $A^0 = 0$. Therefore, these two gauge conditions are effectively equivalent.

Similarly, Eq. (27) by itself does not eliminate 1 degree of freedom. We also need to specify a boundary condition for this differential equation. Since we are not focusing on writing out $A_{\hat{\mu}}$ explicitly, however, we will not dwell on this subject here.

The above discussion should make it clear that Eqs. (26) and (28) are really two sides of the same coin. However, to be consistent with conventions used in the instant form, where the radiation gauge condition is specified as "$A^0 = 0$ and $\nabla\cdot\mathbf{A} = 0$," here we say that the radiation gauge condition for any interpolating angle is Eqs. (26) and (28). In the instant form limit ($\delta = 0$), $A_{\hat{-}} \to A^3, \mathbb{C} \to 1$, and Eq. (28) becomes $\nabla\cdot\mathbf{A} = 0$ while Eq. (26) becomes $A^0 = 0$, which is the familiar Coulomb gauge. In the light-front limit ($\delta = \pi/4$), $A_{\hat{-}} \to A^+, \mathbb{C} \to 0$, and the gauge conditions reduce to "$A^+ = 0$ and $\partial^+A^+ = 0$," which is just $A^+ = 0$, i.e., the light-front gauge.

C. Propagator for transverse photons

Choosing the transverse gauge fields as the dynamical degrees of freedom, we get the photon propagator in the interpolating transverse gauge given by

$$\langle 0|T(A_{\hat{\mu}}(y)A_{\hat{\nu}}(x))|0\rangle = i\int\frac{d^4q}{(2\pi)^4}e^{-iq(y-x)}\frac{\mathcal{T}_{\hat{\mu}\hat{\nu}}}{q^2+i\epsilon}, \tag{31}$$

where $\mathcal{T}_{\hat{\mu}\hat{\nu}} \equiv \sum_{\lambda=\pm}\epsilon^*_{\hat{\mu}}(\lambda)\epsilon_{\hat{\nu}}(\lambda)$ and $\epsilon_{\hat{\mu}}(\lambda) = \epsilon_{\hat{\mu}}(q,\lambda)$ taking the photon momentum $P = q$. Here, we use the obvious familiar notation $q^2 = q_{\hat{\mu}}q^{\hat{\mu}}$. Although we can compute $\mathcal{T}_{\hat{\mu}\hat{\nu}}$ directly using Eqs. (22a) and (22b) as shown in Appendix B, we demonstrate here the method of vierbein as a cross-check to our result.

To construct a vierbein, we just need a temporal basis 4-vector and a longitudinal basis 4-vector that we denote as $\mathring{n}_{\hat{\mu}}$ and $\mathring{q}_{\hat{\mu}}$, respectively, since the transverse basis 4-vectors are already given by $\epsilon_{\hat{\mu}}(\pm)$. The temporal basis 4-vector can be taken as a unit timelike 4-vector given by $\mathring{n}_{\hat{\mu}} = \frac{1}{\sqrt{\mathbb{C}}}n_{\hat{\mu}} = \frac{1}{\sqrt{\mathbb{C}}}(1,0,0,0)$, the dual vector of which is $\mathring{n}^{\hat{\mu}} = (\sqrt{\mathbb{C}},0,0,\mathbb{S}/\sqrt{\mathbb{C}})$. The $\frac{1}{\sqrt{\mathbb{C}}}$ in $n_{\hat{\mu}}$ is a normalization factor to get $\mathring{n}_{\hat{\mu}}\mathring{n}^{\hat{\mu}} = 1$. The longitudinal basis 4-vector $\mathring{q}_{\hat{\mu}}$ can also be rather easily found from the gauge condition given by Eq. (25), which can be written as $\epsilon_{\hat{\mu}}(\lambda)\mathring{q}^{\hat{\mu}} = 0$ with $\mathring{q}^{\hat{\mu}} = N(0,-q_1\mathbb{C},-q_2\mathbb{C},-q_{\hat{-}})$. The normalization factor N is determined by $\mathring{q}_{\hat{\mu}}\mathring{q}^{\hat{\mu}} = \mathring{q}^{\hat{\mu}}g_{\hat{\mu}\hat{\nu}}\mathring{q}^{\hat{\nu}} = -1$ with $g_{\hat{\mu}\hat{\nu}}$ given by Eq. (4), so we have

$$\mathring{q}^{\hat{\mu}} = \frac{1}{\sqrt{\mathbb{C}(\mathbf{q}_\perp^2\mathbb{C} + q_{\hat{-}}^2)}}(0,-q_1\mathbb{C},-q_2\mathbb{C},-q_{\hat{-}}) \tag{32}$$

and

$$\mathring{q}_{\hat{\mu}} = \frac{1}{\sqrt{\mathbb{C}(\mathbf{q}_\perp^2\mathbb{C} + q_{\hat{-}}^2)}}(-\mathbb{S}q_{\hat{-}},q_1\mathbb{C},q_2\mathbb{C},q_{\hat{-}}\mathbb{C}). \tag{33}$$

These four basis 4-vectors are of course mutually orthogonal; i.e., $\mathring{q}_{\hat{\mu}}\mathring{n}^{\hat{\mu}} = 0$, $\epsilon_{\hat{\mu}}(\lambda)\mathring{n}^{\hat{\mu}} = 0$ and $\epsilon_{\hat{\mu}}(\lambda)\mathring{q}^{\hat{\mu}} = 0$, where $\lambda = \pm$.

Since $\epsilon_{\hat{\mu}}(\pm), \mathring{n}_{\hat{\mu}}$, and $\mathring{q}_{\hat{\mu}}$ form a vierbein, we may start from

$$g_{\hat{\mu}\hat{\nu}} = \mathring{n}_{\hat{\mu}}\mathring{n}_{\hat{\nu}} - \sum_{\lambda=\pm}\epsilon^*_{\hat{\mu}}(\lambda)\epsilon_{\hat{\nu}}(\lambda) - \mathring{q}_{\hat{\mu}}\mathring{q}_{\hat{\nu}} \tag{34}$$

and obtain

$$\begin{aligned}\mathcal{T}_{\hat{\mu}\hat{\nu}} &\equiv \sum_{\lambda=\pm}\epsilon^*_{\hat{\mu}}(\lambda)\epsilon_{\hat{\nu}}(\lambda)\\ &= -g_{\hat{\mu}\hat{\nu}} + \mathring{n}_{\hat{\mu}}\mathring{n}_{\hat{\nu}} - \mathring{q}_{\hat{\mu}}\mathring{q}_{\hat{\nu}}\\ &= -g_{\hat{\mu}\hat{\nu}} + \frac{(q\cdot n)(q_{\hat{\mu}}n_{\hat{\nu}} + q_{\hat{\nu}}n_{\hat{\mu}})}{\mathbf{q}_\perp^2\mathbb{C} + q_{\hat{-}}^2}\\ &\quad - \frac{\mathbb{C}q_{\hat{\mu}}q_{\hat{\nu}}}{\mathbf{q}_\perp^2\mathbb{C} + q_{\hat{-}}^2} - \frac{q^2 n_{\hat{\mu}}n_{\hat{\nu}}}{\mathbf{q}_\perp^2\mathbb{C} + q_{\hat{-}}^2},\end{aligned} \tag{35}$$

where we used $\mathring{n}_{\hat{\mu}} = \frac{1}{\sqrt{\mathbb{C}}}n_{\hat{\mu}}$ and rewrote $\mathring{q}_{\hat{\mu}}$ in terms of $q_{\hat{\mu}}$ and $n_{\hat{\mu}}$ as

$$\mathring{q}_{\hat{\mu}} = \frac{\mathbb{C}q_{\hat{\mu}} - (q\cdot n)n_{\hat{\mu}}}{\sqrt{\mathbb{C}(\mathbf{q}_\perp^2\mathbb{C} + q_{\hat{-}}^2)}} \tag{36}$$

in the last step to remove any artifact of divergence in $\mathring{q}_{\hat{\mu}}$ and $\mathring{n}_{\hat{\mu}}$ in the light-front limit. The photon propagator constructed out of $n_{\hat{\mu}}$ and $q_{\hat{\mu}}$ interpolates smoothly and correctly to the one corresponding to the light-front gauge.

In the instant form limit, $\mathbb{C} \to 1$, $\mathbf{q}_\perp^2\mathbb{C} + q_{\hat{-}}^2 \to \mathbf{q}^2 = (q\cdot n)^2 - q^2$, and this reduces to the well-known photon propagator in the Coulomb gauge ($\nabla\cdot\mathbf{A} = 0$) [31],

$$\begin{aligned}\mathcal{T}_{\mu\nu} &= -\eta_{\mu\nu} + \frac{(q\cdot n)(q_\mu n_\nu + q_\nu n_\mu)}{(q\cdot n)^2 - q^2}\\ &\quad - \frac{q_\mu q_\nu}{(q\cdot n)^2 - q^2} - \frac{q^2 n_\mu n_\nu}{(q\cdot n)^2 - q^2},\end{aligned} \tag{37}$$

where $\eta_{\mu\nu} = \mathrm{diag}(1,-1,-1,-1)$ and μ and ν run for 0, 1, 2, 3.

In the light-front limit, $\mathbb{C} \to 0$, $q_{\hat{-}}^2 \to q^{+2} = (q\cdot n)^2$, and this becomes precisely the photon propagator under the light-front gauge ($A^+ = 0$), and we have

$$\mathcal{T}_{\mu\nu} = -g_{\mu\nu} + \frac{(q\cdot n)(q_\mu n_\nu + q_\nu n_\mu)}{(q\cdot n)^2} - \frac{q^2 n_\mu n_\nu}{(q\cdot n)^2}, \tag{38}$$

where $g_{\mu\nu}$ is given by Eq. (4) with $\delta = \pi/4$ and μ and ν run for $+, 1, 2, -$. From this derivation, we see that the appropriate photon propagator for the interpolating gauge given by Eqs. (26) and (27) [or Eq. (28)] has three terms, consistent with Refs. [25–27]. As we will see in the next section, the last term in Eq. (38) is canceled by the instantaneous interaction. Therefore, the two-term gauge propagator [8] can be used effectively without involving the instantaneous interaction.

D. Longitudinal photons

Having used the transverse gauge fields as the dynamical degrees of the freedom, we are left with the longitudinal degree of freedom that also deserves a physical interpretation. This leftover longitudinal degree of freedom is necessary to describe the virtual photon. First, to find the longitudinal polarization ($\lambda = 0$) of the virtual photon, we need to generalize Eq. (22c), replacing M^2 by $P^{\hat{\mu}}P_{\hat{\mu}} = q^2$, which can be either positive (timelike) or negative (spacelike). From the direct computation shown in Appendix B with this replacement, we find

$$\begin{aligned}\mathcal{L}_{\hat{\mu}\hat{\nu}} &\equiv \epsilon^*_{\hat{\mu}}(0)\epsilon_{\hat{\nu}}(0)\\ &= -\frac{(q\cdot n)(q_{\hat{\mu}}n_{\hat{\nu}} + q_{\hat{\nu}}n_{\hat{\mu}})}{\mathbf{q}_\perp^2\mathbb{C} + q_{\hat{-}}^2}\\ &\quad + \frac{(q^{\hat{+}})^2 q_{\hat{\mu}}q_{\hat{\nu}}}{(q)^2(\mathbf{q}_\perp^2\mathbb{C} + q_{\hat{-}}^2)} + \frac{q^2 n_{\hat{\mu}}n_{\hat{\nu}}}{\mathbf{q}_\perp^2\mathbb{C} + q_{\hat{-}}^2}.\end{aligned} \tag{39}$$

Together with $\mathcal{T}_{\hat{\mu}\hat{\nu}}$ given by Eq. (35), it verifies the well-known completeness relation [31]

$$\mathcal{T}_{\hat{\mu}\hat{\nu}} + \mathcal{L}_{\hat{\mu}\hat{\nu}} = -g_{\hat{\mu}\hat{\nu}} + \frac{q_{\hat{\mu}}q_{\hat{\nu}}}{q^2}. \tag{40}$$

We note that the last term in Eq. (39) without the dependence on $q_{\hat{\mu}}$ or $q_{\hat{\nu}}$ provides the instantaneous contribution. As we show in the next section, the instantaneous interaction appearing in the transverse gauge corresponds to the contribution from the longitudinal polarization.

IV. TIME-ORDERED PHOTON EXCHANGE

As Kogut and Soper [32] regarded the theory of quantum electrodynamics as being defined by the usual perturbation expansion of the S matrix in Feynman diagrams, we rewrite the sQED theory here by systematically decomposing each covariant Feynman diagram into a sum of interpolating $x^{\hat{+}}$-ordered diagrams. Since we consider the Feynman expansion as a formal expansion as Kogut and Soper did, we also shall not be concerned in this paper with the convergence of the perturbation series, or convergence and regularization of the integrals.

For clarity, we split this section into three subsections. In the first subsection, we decompose the covariant photon propagator in an arbitrary interpolation angle as a sum of $x^{\hat{+}}$-ordered terms. In the second part, we use the obtained propagator to derive the $x^{\hat{+}}$-ordered diagrams and their amplitudes for the lowest-order photon exchange process. In the final subsection, we verify the invariance of the corresponding total amplitude and discuss about the instant form and light-front limits of the $x^{\hat{+}}$-ordered photon propagators.

A. Photon propagator decomposition

The completeness relation given by Eq. (40) corresponds to the numerator of the covariant photon propagator in the Landau gauge. We start from the covariant photon propagator in position space:

$$D_F(x)_{\hat{\mu}\hat{\nu}} = \int \frac{d^4q}{(2\pi)^4} \frac{-ig_{\hat{\mu}\hat{\nu}} + i\frac{q_{\hat{\mu}}q_{\hat{\nu}}}{q^2}}{q^{\hat{\mu}}q_{\hat{\mu}} + i\epsilon} e^{-iq_{\hat{\mu}}x^{\hat{\mu}}}. \tag{41}$$

Because of the current conservation, however, the term involving $q_{\hat{\mu}}$ does not contribute to any physical process, and our starting point is equivalent to the Feynman photon propagator that Kogut and Soper used for their starting point [32]. For the same reason, the first and second terms that involve $q_{\hat{\mu}}$ can be dropped in Eq. (39), and the covariant photon propagator can be written as

$$\begin{aligned} D_F(x)_{\hat{\mu}\hat{\nu}} &= i\int \frac{d^4q}{(2\pi)^4} \frac{\mathcal{T}_{\hat{\mu}\hat{\nu}}}{q^{\hat{\mu}}q_{\hat{\mu}} + i\epsilon} e^{-iq_{\hat{\mu}}x^{\hat{\mu}}} + \int \frac{d^4q}{(2\pi)^4} \frac{n_{\hat{\mu}}n_{\hat{\nu}}}{\mathbf{q}_\perp^2\mathbb{C} + q_{\hat{-}}^2} e^{-iq_{\hat{\mu}}x^{\hat{\mu}}} \\ &= \int \frac{d^2\mathbf{q}_\perp dq_{\hat{-}} dq_{\hat{+}}}{(2\pi)^4} \exp[-i(q_{\hat{+}}x^{\hat{+}} + q_{\hat{-}}x^{\hat{-}} + \mathbf{q}_\perp\mathbf{x}^\perp)] \left[\frac{i\mathcal{T}_{\hat{\mu}\hat{\nu}}}{\mathbb{C}q_{\hat{+}}^2 + 2\mathbb{S}q_{\hat{-}}q_{\hat{+}} - \mathbb{C}q_{\hat{-}}^2 - \mathbf{q}_\perp^2 + i\epsilon} + \frac{in_{\hat{\mu}}n_{\hat{\nu}}}{\mathbf{q}_\perp^2\mathbb{C} + q_{\hat{-}}^2}\right], \end{aligned} \tag{42}$$

where we used Eq. (8) for $q^{\hat{\mu}}q_{\hat{\mu}}$ in the denominator.

To get the $x^{\hat{+}}$-ordered contributions, we now evaluate the $q_{\hat{+}}$ integral in Eq. (42). We note here that the case of $\mathbb{C} = 0$ should be distinguished from the case of $\mathbb{C} \neq 0$ because the pole structures in the $\mathcal{T}_{\hat{\mu}\hat{\nu}}$ term of Eq. (42) are different between the two cases, i.e., a single pole for $\mathbb{C} = 0$ vs two poles for $\mathbb{C} \neq 0$.

For $\mathbb{C} \neq 0$, the $\mathcal{T}_{\hat{\mu}\hat{\nu}}$ term of Eq. (42) has two poles at

$$A - i\epsilon' = \left(-\mathbb{S}q_{\hat{-}} + \sqrt{q_{\hat{-}}^2 + \mathbb{C}\mathbf{q}_\perp^2}\right)/\mathbb{C} - i\epsilon', \tag{43a}$$

$$B + i\epsilon' = \left(-\mathbb{S}q_{\hat{-}} - \sqrt{q_{\hat{-}}^2 + \mathbb{C}\mathbf{q}_\perp^2}\right)/\mathbb{C} + i\epsilon', \tag{43b}$$

where $\epsilon' > 0$. In calculating the contour integration, we close the contour in the lower (upper) half-plane for $x^{\hat{+}} > 0$ ($x^{\hat{+}} < 0$). This produces a term proportional to the step function $\Theta(x^{\hat{+}})$ and the other term proportional to $\Theta(-x^{\hat{+}})$. We then make changes of the variables $\mathbf{q}_\perp \to -\mathbf{q}_\perp$ and $q_{\hat{-}} \to -q_{\hat{-}}$ which lead to $B \to -A$ for the $\Theta(-x^{\hat{+}})$ term and simplify the result expressing $q_{\hat{+}}$ in terms of A. The last term in Eq. (42) immediately gives a delta function of $x^{\hat{+}}$ after the $q_{\hat{+}}$ integration and provides the instantaneous contribution. We note that the instantaneous contribution stems from the longitudinal polarization of the virtual photon. Putting all terms together, we obtain the result for the case of $\mathbb{C} \neq 0$,

$$\begin{aligned} D_F(x)_{\hat{\mu}\hat{\nu}} &= \int \frac{d^2\mathbf{q}_\perp}{(2\pi)^3} \int_{-\infty}^{\infty} dq_{\hat{-}} \frac{\mathcal{T}_{\hat{\mu}\hat{\nu}}}{2\sqrt{q_{\hat{-}}^2 + \mathbb{C}\mathbf{q}_\perp^2}} [\Theta(x^{\hat{+}})e^{-iq_{\hat{\mu}}x^{\hat{\mu}}} + \Theta(-x^{\hat{+}})e^{iq_{\hat{\mu}}x^{\hat{\mu}}}] \\ &\quad + i\delta(x^{\hat{+}}) \int \frac{d^2\mathbf{q}_\perp}{(2\pi)^3} \int_{-\infty}^{\infty} dq_{\hat{-}} \frac{n_{\hat{\mu}}n_{\hat{\nu}}}{\mathbf{q}_\perp^2\mathbb{C} + q_{\hat{-}}^2} e^{-i(q_{\hat{-}}x^{\hat{-}} + \mathbf{q}_\perp\mathbf{x}^\perp)}, \end{aligned} \tag{44}$$

where $q_{\hat{+}}$ in the exponent of the first two terms should be taken as A given by Eq. (43a).

Now let us look at the light-front case. Because $\mathbb{C} = 0$, there is only one pole at $\mathbf{q}_\perp^2/2q_{\hat{-}} - i\epsilon/2q_{\hat{-}} = \mathbf{q}_\perp^2/2q^+ - i\epsilon/2q^+$. It depends on the sign of q^+ whether this pole is in the upper half-plane or the lower half-plane. As the integration over q^- needs to be done in $q^+ > 0$ and $q^+ < 0$ regions separately, each region will get a step function after closing the contour in the plane where the arc contribution is absent. We again make changes of the variables $q^+ \to -q^+$ and $\mathbf{q}_\perp \to -\mathbf{q}_\perp$ in the term proportional to $\Theta(-x^+)$. We then obtain the result at the light-front [32],

$$D_F(x)_{\mu\nu} = \int \frac{d^2\mathbf{q}_\perp}{(2\pi)^3} \int_0^{\infty} \frac{dq^+}{2q^+} \mathcal{T}_{\mu\nu}[\Theta(x^+)e^{-iq_\mu x^\mu} + \Theta(-x^+)e^{iq_\mu x^\mu}] + i\delta(x^+) \int \frac{d^2\mathbf{q}_\perp}{(2\pi)^3} \int_{-\infty}^{\infty} dq^+ \frac{n_\mu n_\nu}{(q^+)^2} e^{-i(q^+x^- - \mathbf{q}^\perp\mathbf{x}^\perp)}, \tag{45}$$

where the indices μ and ν run for $+, 1, 2, -$ and q^- in the exponent of the first two terms should be taken as $\mathbf{q}_\perp^2/2q^+$. More details of the derivation for this equation can be found in Appendix C.

We note that the result for $\mathbb{C} \neq 0$ given by Eq. (44) does not coincide with the result for $\mathbb{C} = 0$ given by Eq. (45) as we take the limit $\mathbb{C} \to 0$, because the integration range $(-\infty\ \infty)$ in $q_{\hat{-}}$ is different from the integration range $(0, \infty)$ in q^+ due to the difference in the pole structure between the two cases, $\mathbb{C} \neq 0$ and $\mathbb{C} = 0$, as we mentioned earlier. Nevertheless, it can be written in a unified form by introducing an interpolating step function $\hat{\Theta}(q_{\hat{-}})$ given by

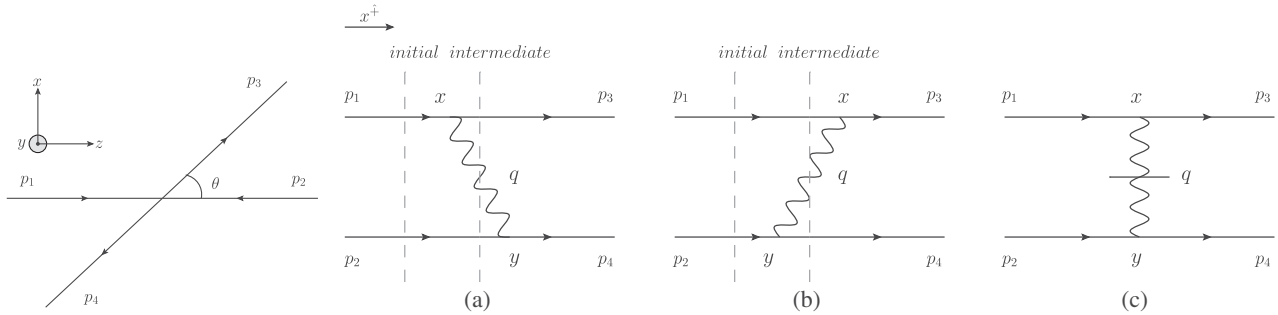

FIG. 1. The scattering of two particles in their center-of-mass frame (leftmost figure) and the three corresponding $x^{\hat{+}}$-ordered diagrams.

$$\hat{\Theta}(q_{\hat{-}}) = \Theta(q_{\hat{-}}) + (1-\delta_{\mathbb{C}0})\Theta(-q_{\hat{-}}) = \begin{cases} 1 & (\mathbb{C} \neq 0) \\ \Theta(q^+) & (\mathbb{C} = 0) \end{cases} \tag{46}$$

and realizing that A given by Eq. (43a) coincides with $q^- = \mathbf{q}_\perp^2/2q^+$ in the limit $\mathbb{C} \to 0$, i.e.,

$$D_F(x)_{\hat{\mu}\hat{\nu}} = \int \frac{d^2\mathbf{q}_\perp}{(2\pi)^3} \int_{-\infty}^{\infty} dq_{\hat{-}} \hat{\Theta}(q_{\hat{-}}) \frac{\mathcal{T}_{\hat{\mu}\hat{\nu}}}{2\sqrt{q_{\hat{-}}^2 + \mathbb{C}\mathbf{q}_\perp^2}} [\Theta(x^{\hat{+}}) e^{-iq_{\hat{\mu}}x^{\hat{\mu}}} + \Theta(-x^{\hat{+}}) e^{iq_{\hat{\mu}}x^{\hat{\mu}}}] + i\delta(x^{\hat{+}}) \int \frac{d^2\mathbf{q}_\perp}{(2\pi)^3} \int_{-\infty}^{\infty} dq_{\hat{-}} \frac{n_{\hat{\mu}} n_{\hat{\nu}}}{\mathbf{q}_\perp^2 \mathbb{C} + q_{\hat{-}}^2} e^{-i(q_{\hat{-}}x^{\hat{-}} + \mathbf{q}_\perp \mathbf{x}^\perp)}, \tag{47}$$

where again $q_{\hat{+}}$ in the exponent of the first two terms should be taken as A given by Eq. (43a). From now on, we will use Eq. (47) for all interpolation angles including $\mathbb{C} = 0$.

B. Time-ordered diagrams

The Lagrangian for sQED can be written as

$$\mathcal{L} = D_\mu \phi D^\mu \phi^* - m^2 \phi^* \phi - \frac{1}{4} F^{\mu\nu} F_{\mu\nu} = \partial_\mu \phi \partial^\mu \phi^* - m^2 \phi^* \phi - \frac{1}{4} F^{\mu\nu} F_{\mu\nu} - e J^\mu A_\mu + e^2 A_\mu A^\mu \phi^* \phi, \tag{48}$$

where

$$D_\mu = \partial_\mu + ieA_\mu, \tag{49}$$

$$J^\mu = -i(\phi \partial^\mu \phi^* - \phi^* \partial^\mu \phi). \tag{50}$$

To examine the contribution of each term in Eq. (47), we compute the lowest-order tree-level scattering amplitude starting from the usual Feynman amplitude in coordinate space. For the lowest tree-level scattering diagram, $e^2 A_\mu A^\mu \phi^* \phi$ does not contribute, and the amplitude can be written as

$$i\mathcal{M} = (-ie)^2 \int d^4x d^4y [J^{\hat{\mu}}(y) D_F(y-x)_{\hat{\mu}\hat{\nu}} J^{\hat{\nu}}(x)]. \tag{51}$$

The scalar wave functions used here are the plane waves

$$\phi(x) = e^{-ip_{\hat{\mu}}x^{\hat{\mu}}}. \tag{52}$$

For a specific scattering process shown in Fig. 1, the currents from p_1 to p_3 and from p_2 to p_4 are, respectively, given by

$$J^{\hat{\nu}} = -i(\phi_1 \partial^{\hat{\nu}} \phi_3^* - \phi_3^* \partial^{\hat{\nu}} \phi_1) = (p_1^{\hat{\nu}} + p_3^{\hat{\nu}}) e^{i(p_3 - p_1)x}, \tag{53}$$

$$J^{\hat{\mu}} = -i(\phi_2 \partial^{\hat{\mu}} \phi_4^* - \phi_4^* \partial^{\hat{\mu}} \phi_2) = (p_2^{\hat{\mu}} + p_4^{\hat{\mu}}) e^{i(p_4 - p_2)y}. \tag{54}$$

With the change of variables

$$x \to x, \qquad y \to T = y - x, \tag{55}$$

Eq. (51) becomes

$$i\mathcal{M} = (-ie)^2 \int d^4x d^4T e^{i(p_4 - p_2)T} e^{i(p_4 + p_3 - p_2 - p_1)x} \times (p_2^{\hat{\mu}} + p_4^{\hat{\mu}}) D_{\hat{\mu}\hat{\nu}}(T) (p_1^{\hat{\nu}} + p_3^{\hat{\nu}}). \tag{56}$$

The x integration resulting in $(2\pi)^4 \delta^4(p_4 + p_3 - p_2 - p_1)$ provides the total energy and momentum conservation. For

the T integration, we use $D_{\hat{\mu}\hat{\nu}}$ given by Eq. (47) as well as the following relations:

$$\int_{-\infty}^{\infty} dT^{\hat{+}}\Theta(T^{\hat{+}})e^{iP_{\hat{+}}T^{\hat{+}}} = \frac{i}{P_{\hat{+}}}, \tag{57}$$

$$\int_{-\infty}^{\infty} dT^{\hat{+}}\Theta(-T^{\hat{+}})e^{iP_{\hat{+}}T^{\hat{+}}} = -\frac{i}{P_{\hat{+}}}, \tag{58}$$

$$\int_{-\infty}^{\infty} dT^{\hat{+}}e^{iP_{\hat{+}}T^{\hat{+}}} = 2\pi\delta(P_{\hat{+}}). \tag{59}$$

After the x and T integration, we get

$$i\mathcal{M} = (-ie)^2(p_4^{\hat{\mu}} + p_2^{\hat{\mu}})\Pi_{\hat{\mu}\hat{\nu}}(p_3^{\hat{\nu}} + p_1^{\hat{\nu}}) \times (2\pi)^4\delta^4(p_4 + p_3 - p_2 - p_1), \tag{60}$$

where

$$\begin{aligned}\Pi_{\hat{\mu}\hat{\nu}} = \int \frac{d^2\mathbf{q}_\perp dq_{\hat{-}}\hat{\Theta}(q_{\hat{-}})}{2\sqrt{q_{\hat{-}}^2 + \mathbb{C}\mathbf{q}_\perp^2}} &\left[\frac{i\mathcal{T}_{\hat{\mu}\hat{\nu}}}{p_{4\hat{+}} - p_{2\hat{+}} - A}\delta(p_{4\hat{-}} - p_{2\hat{-}} - q_{\hat{-}})\delta^2(\mathbf{p}_{4\perp} - \mathbf{p}_{2\perp} - \mathbf{q}_\perp)\right.\\ &\left. - \frac{i\mathcal{T}_{\hat{\mu}\hat{\nu}}}{p_{4\hat{+}} - p_{2\hat{+}} + A}\delta(p_{4\hat{-}} - p_{2\hat{-}} + q_{\hat{-}})\delta^2(\mathbf{p}_{4\perp} - \mathbf{p}_{2\perp} + \mathbf{q}_\perp)\right]\\ &+ \int d^2\mathbf{q}_\perp dq_{\hat{-}} \frac{in_{\hat{\mu}}n_{\hat{\nu}}}{\mathbf{q}_\perp^2\mathbb{C} + q_{\hat{-}}^2}\delta(p_{4\hat{-}} - p_{2\hat{-}} - q_{\hat{-}})\delta^2(\mathbf{p}_{4\perp} - \mathbf{p}_{2\perp} - \mathbf{q}_\perp).\end{aligned} \tag{61}$$

The three terms in $\Pi_{\hat{\mu}\hat{\nu}}$ corresponds to three different "time" orderings $y^{\hat{+}} > x^{\hat{+}}$, $y^{\hat{+}} < x^{\hat{+}}$ and $y^{\hat{+}} = x^{\hat{+}}$, respectively.[1] The associated delta functions provide the momentum conservation at each vertex as well as the conservation of total energy and momentum between the initial and final particles. In Fig. 1, the three "time" -ordered diagrams are depicted with the momentum conservation at each vertex.

The corresponding photon propagators for $T^{\hat{+}} > 0$ (or $y^{\hat{+}} > x^{\hat{+}}$) and $T^{\hat{+}} < 0$ (or $y^{\hat{+}} < x^{\hat{+}}$) are, respectively, given by

$$\begin{aligned}\Pi_{\hat{\mu}\hat{\nu}}^{(a)} &= \frac{1}{2Q^{\hat{+}(a)}}\frac{i\mathcal{T}_{\hat{\mu}\hat{\nu}}\hat{\Theta}(p_{4\hat{-}} - p_{2\hat{-}})}{p_{4\hat{+}} - p_{2\hat{+}} - Q_{\hat{+}}^{(a)}}\\ &= \frac{1}{2Q^{\hat{+}(a)}}\frac{i\mathcal{T}_{\hat{\mu}\hat{\nu}}\hat{\Theta}(p_{1\hat{-}} - p_{3\hat{-}})}{p_{1\hat{+}} - p_{3\hat{+}} - Q_{\hat{+}}^{(a)}},\end{aligned} \tag{62}$$

and

$$\begin{aligned}\Pi_{\hat{\mu}\hat{\nu}}^{(b)} &= -\frac{1}{2Q^{\hat{+}(b)}}\frac{i\mathcal{T}_{\hat{\mu}\hat{\nu}}\hat{\Theta}(p_{2\hat{-}} - p_{4\hat{-}})}{p_{4\hat{+}} - p_{2\hat{+}} + Q_{\hat{+}}^{(b)}}\\ &= \frac{1}{2Q^{\hat{+}(b)}}\frac{i\mathcal{T}_{\hat{\mu}\hat{\nu}}\hat{\Theta}(p_{2\hat{-}} - p_{4\hat{-}})}{p_{2\hat{+}} - p_{4\hat{+}} - Q_{\hat{+}}^{(b)}}\\ &= \frac{1}{2Q^{\hat{+}(b)}}\frac{i\mathcal{T}_{\hat{\mu}\hat{\nu}}\hat{\Theta}(p_{3\hat{-}} - p_{1\hat{-}})}{p_{3\hat{+}} - p_{1\hat{+}} - Q_{\hat{+}}^{(b)}},\end{aligned} \tag{63}$$

where

$$Q^{\hat{+}(i)} = \sqrt{[q_{\hat{-}}^{(i)}]^2 + \mathbb{C}[\mathbf{q}_\perp^{(i)}]^2}, \qquad (i = a, b) \tag{64}$$

$$Q_{\hat{+}}^{(i)} = \frac{-\mathbb{S}q_{\hat{-}}^{(i)} + \sqrt{[q_{\hat{-}}^{(i)}]^2 + \mathbb{C}[\mathbf{q}_\perp^{(i)}]^2}}{\mathbb{C}}, \qquad (i = a, b) \tag{65}$$

and

$$q_{\hat{-}}^{(a)} = -q_{\hat{-}}^{(b)} = p_{1\hat{-}} - p_{3\hat{-}}, \tag{66}$$

$$\mathbf{q}_\perp^{(a)} = -\mathbf{q}_\perp^{(b)} = \mathbf{p}_{1\perp} - \mathbf{p}_{3\perp}. \tag{67}$$

The total energy-momentum conservation in Eq. (60) as well as the momentum conservation at each vertex were used here. $Q_{\hat{+}}^{(i)}$ and $Q^{\hat{+}(i)}$ satisfy the on-mass-shell condition of the propagating photon with momentum $(q_{\hat{-}}^{(i)}, \mathbf{q}_\perp^{(i)})$. To see this, one can use Eq. (10) for a massless photon to derive the $Q^{\hat{+}}$ in terms of $q_{\hat{-}}$ and $\mathbf{q}_\perp$, noting that $Q^{\hat{+}}$ is positive definite for an on-mass-shell particle due to Eq. (6a). The formula for $Q_{\hat{+}}$ can also be obtained in terms of $Q_{\hat{-}}$ and $Q^{\hat{+}}$ by using Eq. (7). Equations (62) and (63) can then be written in a unified form,[2]

$$\Pi_{\hat{\mu}\hat{\nu}}^{(i)} = \frac{1}{2Q^{\hat{+}(i)}}\frac{i\mathcal{T}_{\hat{\mu}\hat{\nu}}\hat{\Theta}(q_{\hat{-}}^{(i)})}{P_{\mathrm{ini}\hat{+}} - P_{\mathrm{inter}\hat{+}}}, \qquad (i = a, b), \tag{68}$$

[1]In this paper, the time means the generalized interpolation time $x^{\hat{+}}$ unless specified otherwise.

[2]Note that the subscripts $\hat{+}$ and $\hat{-}$ denote the energy and the longitudinal momentum for a given interpolating momentum, respectively.

where $P_{\mathrm{ini}\hat{+}}$ [$P_{\mathrm{inter}\hat{+}}$] is the sum of the energy of the initial (intermediate) particles. All the initial and intermediate particles are now on their mass shells. This agrees with the familiar time-ordered perturbation theory in the IFD, although we now see it as a generalization to any interpolation angle. We note here that the propagating photon as the dynamical degree of freedom has only the transverse polarization. This is consistent with the interpretation that the intermediate particles are now "on-mass-shell" or "physical."

Besides the two propagating terms, there is a third term in Eq. (61) that represents the instantaneous contribution. For the sake of consistency in our notation, we denote this part of $\Pi_{\hat{\mu}\hat{\nu}}$ as

$$\Pi^{(c)}_{\hat{\mu}\hat{\nu}} = \frac{i n_{\hat{\mu}} n_{\hat{\nu}}}{\mathbf{q}_\perp^2 \mathbb{C} + q_{\hat{-}}^2}, \tag{69}$$

where $q_{\hat{-}}$ and $\mathbf{q}_\perp$ are given by Eqs. (66) and (67), respectively. As noted earlier, the instantaneous contribution stems from the longitudinal polarization of the virtual photon.

We thus have three time-ordered diagrams as shown in Fig. 1, the first two of which represent time-ordered exchanges of the propagating photon and the third of which represents the instantaneous interaction. The invariant amplitude is then the sum of all three time-ordered amplitudes,

$$\begin{aligned} i\mathcal{M} &= \sum_{j=a,b,c} i\mathcal{M}^{(j)} \\ &= (-ie)^2 \sum_{j=a,b,c} (p_4^{\hat{\mu}} + p_2^{\hat{\mu}}) \Pi^{(j)}_{\hat{\mu}\hat{\nu}} (p_3^{\hat{\nu}} + p_1^{\hat{\nu}}), \end{aligned} \tag{70}$$

where the total energy-momentum conservation factor $(2\pi)^4 \delta^4(p_4 + p_3 - p_2 - p_1)$ is implied.

C. LFD vs the Limit to LFD

Since the time-ordered gauge propagators have the interpolating step function given by Eq. (46), we take a closer look at the limiting cases of $\mathbb{C} \to 0$ and compare the results with the exact $\mathbb{C} = 0$ (LFD) results in this subsection. For convenience and simplicity of our discussion, we drop the (i) superscript in Eq. (64) and have

$$\begin{aligned} Q^{\hat{+}(a)} &= Q^{\hat{+}(b)} \\ &= \sqrt{(p_{1\hat{-}} - p_{3\hat{-}})^2 + (\mathbf{p}_{1\perp} - \mathbf{p}_{3\perp})^2 \mathbb{C}} \equiv Q^{\hat{+}}. \end{aligned} \tag{71}$$

Because the terms proportional to $q_{\hat{\mu}}$ or $q_{\hat{\nu}}$ in $\mathcal{T}_{\hat{\mu}\hat{\nu}}$ can be discarded due to the current conservation in the physical process, we may also replace $\mathcal{T}_{\hat{\mu}\hat{\nu}}$ by

$$\tilde{\mathcal{T}}_{\hat{\mu}\hat{\nu}} \equiv -g_{\hat{\mu}\hat{\nu}} - \frac{q^2 n_{\hat{\mu}} n_{\hat{\nu}}}{\mathbf{q}_\perp^2 \mathbb{C} + q_{\hat{-}}^2}. \tag{72}$$

Then, Eqs. (62), (63), and (69) can be rewritten as

$$\Pi^{(a)}_{\hat{\mu}\hat{\nu}} = \frac{1}{2Q^{\hat{+}}} \frac{i\tilde{\mathcal{T}}_{\hat{\mu}\hat{\nu}} \hat{\Theta}(p_{1\hat{-}} - p_{3\hat{-}})}{p_{1\hat{+}} - p_{3\hat{+}} - Q^{(a)}_{\hat{+}}}, \tag{73a}$$

$$\Pi^{(b)}_{\hat{\mu}\hat{\nu}} = -\frac{1}{2Q^{\hat{+}}} \frac{i\tilde{\mathcal{T}}_{\hat{\mu}\hat{\nu}} \hat{\Theta}(p_{3\hat{-}} - p_{1\hat{-}})}{p_{1\hat{+}} - p_{3\hat{+}} + Q^{(b)}_{\hat{+}}}, \tag{73b}$$

$$\Pi^{(c)}_{\hat{\mu}\hat{\nu}} = \frac{i n_{\hat{\mu}} n_{\hat{\nu}}}{(Q^{\hat{+}})^2}, \tag{73c}$$

where $Q^{(a)}_{\hat{+}}$ and $Q^{(b)}_{\hat{+}}$ are given by Eq. (65).

For $\mathbb{C} \neq 0$, assigning the 4-momentum transfer q as

$$q_{\hat{-}} \equiv p_{1\hat{-}} - p_{3\hat{-}} = q^{(a)}_{\hat{-}} = -q^{(b)}_{\hat{-}}, \tag{74a}$$

$$\mathbf{q}_\perp \equiv \mathbf{p}_{1\perp} - \mathbf{p}_{3\perp} = \mathbf{q}^{(a)}_\perp = -\mathbf{q}^{(b)}_\perp, \tag{74b}$$

$$q_{\hat{+}} \equiv p_{1\hat{+}} - p_{3\hat{+}} = -(p_{2\hat{+}} - p_{4\hat{+}}), \tag{74c}$$

we have

$$Q^{(a)}_{\hat{+}} = \frac{-\mathbb{S} q_{\hat{-}} + \sqrt{q_{\hat{-}}^2 + \mathbb{C}\mathbf{q}_\perp^2}}{\mathbb{C}} = \frac{-\mathbb{S} q_{\hat{-}} + Q^{\hat{+}}}{\mathbb{C}}, \tag{75}$$

$$Q^{(b)}_{\hat{+}} = \frac{\mathbb{S} q_{\hat{-}} + \sqrt{q_{\hat{-}}^2 + \mathbb{C}\mathbf{q}_\perp^2}}{\mathbb{C}} = \frac{\mathbb{S} q_{\hat{-}} + Q^{\hat{+}}}{\mathbb{C}}. \tag{76}$$

Since both $\hat{\Theta}(q_{\hat{-}})$ and $\hat{\Theta}(-q_{\hat{-}})$ are unity for $\mathbb{C} \neq 0$, $\Pi^{(a)}_{\hat{\mu}\hat{\nu}}$ and $\Pi^{(b)}_{\hat{\mu}\hat{\nu}}$ can be rewritten as

$$\Pi^{(a)}_{\hat{\mu}\hat{\nu}} = \frac{1}{2Q^{\hat{+}}} \frac{i\tilde{\mathcal{T}}_{\hat{\mu}\hat{\nu}} \mathbb{C}}{\mathbb{C} q_{\hat{+}} + \mathbb{S} q_{\hat{-}} - Q^{\hat{+}}} = \frac{1}{2Q^{\hat{+}}} \frac{i\tilde{\mathcal{T}}_{\hat{\mu}\hat{\nu}} \mathbb{C}}{q^{\hat{+}} - Q^{\hat{+}}}, \tag{77a}$$

$$\Pi^{(b)}_{\hat{\mu}\hat{\nu}} = -\frac{1}{2Q^{\hat{+}}} \frac{i\tilde{\mathcal{T}}_{\hat{\mu}\hat{\nu}} \mathbb{C}}{\mathbb{C} q_{\hat{+}} + \mathbb{S} q_{\hat{-}} + Q^{\hat{+}}} = -\frac{1}{2Q^{\hat{+}}} \frac{i\tilde{\mathcal{T}}_{\hat{\mu}\hat{\nu}} \mathbb{C}}{q^{\hat{+}} + Q^{\hat{+}}}. \tag{77b}$$

Summing all contributions, we use Eqs. (10), (71), and (72) to verify

$$\Pi^{(a)}_{\hat{\mu}\hat{\nu}} + \Pi^{(b)}_{\hat{\mu}\hat{\nu}} + \Pi^{(c)}_{\hat{\mu}\hat{\nu}} = \frac{i\tilde{\mathcal{T}}_{\hat{\mu}\hat{\nu}}\mathbb{C}}{(q^{\hat{+}})^2 - (Q^{\hat{+}})^2} + \frac{in_{\hat{\mu}}n_{\hat{\nu}}}{\mathbf{q}_\perp^2\mathbb{C} + q_{\hat{-}}^2} = \frac{i\tilde{\mathcal{T}}_{\hat{\mu}\hat{\nu}}}{q^2} + \frac{in_{\hat{\mu}}n_{\hat{\nu}}}{\mathbf{q}_\perp^2\mathbb{C} + q_{\hat{-}}^2} = \frac{-ig_{\hat{\mu}\hat{\nu}}}{q^2}. \tag{78}$$

It is clear from this derivation that the contribution from the instantaneous interaction is cancelled by the corresponding $n_{\hat{\mu}}n_{\hat{\nu}}$ term in the transverse photon propagator and the sum of all the contributions is totally Lorentz invariant.

For $\mathbb{C} = 0$, $\hat{\Theta}(q_{\hat{-}})$ and $\hat{\Theta}(-q_{\hat{-}})$ are neither unity nor the same as each other. Thus, we need to look into the details of each contribution in Eqs. (73a), (73b), and (73c) very carefully to understand the Lorentz invariance of the total amplitude. Taking $\mathbb{C} = 0$ in Eqs. (73a), (73b), and (73c), we get

$$\Pi^{(a)}_{\mu\nu} = \frac{1}{2q^+}\frac{i(-g_{\mu\nu} - \frac{q^2 n_\mu n_\nu}{(q^+)^2})\Theta(q^+)}{p_1^- - p_3^- - \frac{\mathbf{q}_\perp^2}{2q^+}}, \tag{79a}$$

$$\Pi^{(b)}_{\mu\nu} = -\frac{1}{2|q^+|}\frac{i(-g_{\mu\nu} - \frac{q^2 n_\mu n_\nu}{(q^+)^2})\Theta(-q^+)}{p_1^- - p_3^- + \frac{\mathbf{q}_\perp^2}{2|q^+|}}, \tag{79b}$$

$$\Pi^{(c)}_{\mu\nu} = \frac{in_\mu n_\nu}{q^{+2}}, \tag{79c}$$

where $q^+ = p_1^+ - p_3^+$ and of course the conservation of total light-front (LF) energy in the initial and final states is imposed such as $p_1^- - p_3^- = p_4^- - p_2^-$. In this case, the contribution from the LF time-ordered process (a) or (b) in Fig. 1 depends on the values of external momenta p_1^+ and p_3^+, i.e., whether $p_1^+ > p_3^+$ or $p_1^+ < p_3^+$. As indicated by $\Theta(q^+)$ and $\Theta(-q^+)$ in Eqs. (79a) and (79b), once the external kinematic situation is given, only one of these two LF time-ordered processes contributes. For example, if $p_1^+ > p_3^+$, then only (a) contributes. Similarly, if $p_1^+ < p_3^+$, then only (b) contributes. This is dramatically different from the $\mathbb{C} \neq 0$ case in which both (a) and (b) contribute regardless of $p_{1\hat{-}} > p_{3\hat{-}}$ or $p_{1\hat{-}} < p_{3\hat{-}}$. The limiting case $\mathbb{C} \to 0$ will be separately discussed later after this discussion of LFD, i.e., $\mathbb{C} = 0$. Although either (a) or (b) (not both) contributes to the total amplitude, the Lorentz invariance of the total amplitude is assured in LFD. For example, if $p_1^+ > p_3^+$, then the sum of all contributions is given by

$$\Pi^{(a)}_{\mu\nu} + \Pi^{(c)}_{\mu\nu} = \frac{1}{2q^+}\frac{i(-g_{\mu\nu} - \frac{q^2 n_\mu n_\nu}{(q^+)^2})}{p_1^- - p_3^- - \frac{\mathbf{q}_\perp^2}{2q^+}} + \frac{in_\mu n_\nu}{q^{+2}} = \frac{i(-g_{\mu\nu} - \frac{q^2 n_\mu n_\nu}{(q^+)^2})}{2q^+q^- - \mathbf{q}_\perp^2} + \frac{in_\mu n_\nu}{q^{+2}} = \frac{-ig_{\mu\nu}}{q^2}, \tag{80}$$

where $p_1^- - p_3^- = q^-$ since the 4-momentum transfer q is assigned as $p_1 - p_3$. As in the $\mathbb{C} \neq 0$ case, the contribution from the instantaneous interaction is cancelled by the corresponding $n_\mu n_\nu$ term in the transverse photon propagator, and the sum of all the contributions is totally Lorentz invariant. Similarly, if $p_1^+ < p_3^+$, then $\Pi^{(a)}_{\mu\nu}$ is replaced by $\Pi^{(b)}_{\mu\nu}$ with $|q^+| = -q^+$, and the sum $\Pi^{(b)}_{\mu\nu} + \Pi^{(c)}_{\mu\nu} = \frac{-ig_{\mu\nu}}{q^2}$ is totally Lorentz invariant.

Now, let us consider the limit $\mathbb{C} \to 0$ (i.e., $\delta \to \pi/4$ or $\mathbb{S} \to 1$) from the $\mathbb{C} \neq 0$ case given by Eqs. (77a) and (77b), where we take $q_{\hat{+}} \to q_+ = q^-, q_{\hat{-}} \to q_- = q^+$, and $Q^{\hat{+}} \to Q^+ = q^+$. To obtain the correct limits, we need to make a careful expansion. For $q^+ = p_1^+ - p_3^+ > 0$, we get

$$\mathbb{C}q_{\hat{+}} + \mathbb{S}q_{\hat{-}} - Q^{\hat{+}} = \mathbb{C}q_{\hat{+}} + \mathbb{S}q_{\hat{-}} - \sqrt{q_{\hat{-}}^2 + \mathbb{C}\mathbf{q}_\perp^2} \to \mathbb{C}q^- + q^+ - \sqrt{q^{+2} + \mathbb{C}\mathbf{q}_\perp^2} \to \mathbb{C}q^- - \mathbb{C}\frac{\mathbf{q}_\perp^2}{2q^+} + \mathcal{O}(\mathbb{C}^2), \tag{81}$$

$$\mathbb{C}q_{\hat{+}} + \mathbb{S}q_{\hat{-}} + Q^{\hat{+}} \to 2q^+ + \mathbb{C}q_+ + \mathbb{C}\frac{\mathbf{q}_\perp^2}{2q^+} + \mathcal{O}(\mathbb{C}^2), \tag{82}$$

$$\tilde{\mathcal{T}}_{\hat{\mu}\hat{\nu}} \to -g_{\mu\nu} - 2\frac{q^- - \frac{\mathbf{q}_\perp^2}{2q^+}}{q^+}n_\mu n_\nu. \tag{83}$$

Thus, in the limit $\mathbb{C} \to 0$ for $p_1^+ > p_3^+$, Eqs. (77a), (77b), and (73c) become

$$\Pi^{(a)}_{\mu\nu} = \frac{i\tilde{\mathcal{T}}_{\hat{\mu}\hat{\nu}}}{2q^+}\frac{1}{q^- - \frac{\mathbf{q}_\perp^2}{2q^+}} = -i\frac{g_{\mu\nu}}{2q^+}\frac{1}{q^- - \frac{\mathbf{q}_\perp^2}{2q^+}} - i\frac{n_\mu n_\nu}{(q^+)^2}, \tag{84a}$$

$$\Pi^{(b)}_{\mu\nu} = \lim_{\mathbb{C}\to 0}\frac{-i\tilde{\mathcal{T}}_{\hat{\mu}\hat{\nu}}}{2q^+}\frac{\mathbb{C}}{2q^+ + \mathbb{C}q_+ + \mathbb{C}\frac{\mathbf{q}_\perp^2}{q^+}} \to 0, \tag{84b}$$

$$\Pi^{(c)}_{\mu\nu} = \frac{in_\mu n_\nu}{(q^+)^2}. \tag{84c}$$

This shows the agreement between the $\mathbb{C}=0$ result and the $\mathbb{C}\to 0$ result for the kinematic situation $p_1^+ > p_3^+$. Note here that $\Pi_{\mu\nu}^{(b)}=0$ was given in LFD ($\mathbb{C}=0$) via the factor $\Theta(-q^+)$ in Eq. (79b), while $\Pi_{\mu\nu}^{(b)}\to 0$ as $\mathbb{C}\to 0$ in Eq. (84b) is obtained without the factor $\Theta(-q^+)$. Similarly, the agreement between the $\mathbb{C}=0$ result and the $\mathbb{C}\to 0$ result is also found for the kinematic situation $p_1^+ < p_3^+$ following the procedure described above.

Having shown the agreement between the $\mathbb{C}=0$ result and the $\mathbb{C}\to 0$ result for the kinematic situation $p_1^+ \neq p_3^+$, let us now consider the special kinematic situation $p_1^+ = p_3^+$. If this kinematic situation is provided with the nonzero values of p_1^+ and p_3^+, i.e., $p_1^+ = p_3^+ \neq 0$, then the LF time-ordered processes (a) and (b) are indistinguishable, and the results of $\Pi_{\mu\nu}^{(a)}$ and $\Pi_{\mu\nu}^{(b)}$ given by Eqs. (79a) and (79b), respectively, are identical with the factor $\Theta(q^+=-q^+=0)=1/2$. We also find that the limit $\mathbb{C}\to 0$ of Eqs. (77a) and (77b) agree with these results, precisely yielding the $1/2$ factor both for (a) and (b) contributions as in the $\mathbb{C}=0$ result. Thus, both in $\mathbb{C}=0$ and the limit $\mathbb{C}\to 0$, the total amplitude is given by

$$\Pi_{\mu\nu}^{(a)}+\Pi_{\mu\nu}^{(b)}+\Pi_{\mu\nu}^{(c)}=\frac{-ig_{\mu\nu}}{q^2}, \tag{85}$$

where $q^2=-\mathbf{q}_\perp^2$ and the divergent instantaneous interaction is cancelled by the corresponding divergent $n_\mu n_\nu$ term in the transverse photon propagator.

The LFD results at exact $\mathbb{C}=0$ are attainable for all the kinematic regions that we discussed in this subsection so far, i.e., $p_1^+ > p_3^+$, $p_1^+ < p_3^+$, and $p_1^+ = p_3^+ \neq 0$. However, the agreement between the two, i.e., the LFD vs the limit to the LFD, should be looked into more carefully for the case $p_1^+ = p_3^+ = 0$. This special kinematic situation $p_1^+ = p_3^+ = 0$ involves the discussion of the infinite momentum frame (IMF) with $P^z\to -\infty$, since all the plus momenta go to zero in this frame. Presenting the numerical results with the frame dependence of the time-ordered amplitudes in the next section, we will discuss a particular case of correlating the two limits, $\mathbb{C}\to 0$ and $q^+\to 0$, in conjunction with the J-shaped correlation coined in our previous work [21]. As we show in the next section, the results in the limit $\mathbb{C}\to 0$ following the J curve are different from those in the LFD or at the exact $\mathbb{C}=0$.

V. FRAME DEPENDENCE AND INTERPOLATION ANGLE DEPENDENCE OF TIME-ORDERED AMPLITUDES

In this section, we numerically compute the scattering amplitudes shown in Fig. 1 and discuss both the frame dependence and the interpolation angle dependence of each and every $x^{\hat{+}}$-ordered amplitude. Putting Eqs. (73a), (73b), and (73c) back into Eq. (70), we have the time-ordered amplitudes in the form

$$\mathcal{M}^{(a)}=-(-ie)^2\frac{[p_{24}\cdot p_{13}+p_{24}^{\hat{+}}p_{13}^{\hat{+}}q^2/(Q^{\hat{+}})^2]\mathbb{C}\hat{\Theta}(p_{1\hat{-}}-p_{3\hat{-}})}{2Q^{\hat{+}}(q^{\hat{+}}-Q^{\hat{+}})}, \tag{86a}$$

$$\mathcal{M}^{(b)}=(-ie)^2\frac{[p_{24}\cdot p_{13}+p_{24}^{\hat{+}}p_{13}^{\hat{+}}q^2/Q^{\hat{+}})^2]\mathbb{C}\hat{\Theta}(p_{3\hat{-}}-p_{1\hat{-}})}{2Q^{\hat{+}}(q^{\hat{+}}+Q^{\hat{+}})}, \tag{86b}$$

$$\mathcal{M}^{(c)}=(-ie)^2\frac{p_{24}^{\hat{+}}p_{13}^{\hat{+}}}{(Q^{\hat{+}})^2}, \tag{86c}$$

where

$$p_{24}=p_2+p_4, \tag{87a}$$

$$p_{13}=p_1+p_3. \tag{87b}$$

As we have shown in the last section, the sum of these three $x^{\hat{+}}$-ordered amplitudes agrees with the manifestly invariant total amplitude regardless of whether $\mathbb{C}\neq 0$ or $\mathbb{C}=0$:

$$\mathcal{M}=\Sigma_{j=a,b,c}\mathcal{M}^{(j)}=-(-ie)^2\frac{p_{24}p_{13}}{q^2}. \tag{88}$$

To investigate the frame dependence of these amplitudes, we first look at how they change under different transformations. From Eq. (16a), one can see that, when $\beta_3=0$, $T_{12}^\dagger P^{\hat{+}}T_{12}=P^{\hat{+}}$. So under the kinematic transformation T_{12}, all the $\hat{+}$ components, namely, $q^{\hat{+}}$, $Q^{\hat{+}}$, $p_{13}^{\hat{+}}$, and $p_{24}^{\hat{+}}$, remain the same. We also note that the factors of

$\hat{\Theta}(p_{1\hat{-}} - p_{3\hat{-}})$ and $\hat{\Theta}(p_{3\hat{-}} - p_{1\hat{-}})$ are invariant under T_{12} because these factors are unity for $\mathbb{C} \neq 0$ and become $\Theta(p_1^+ - p_3^+)$ and $\Theta(p_3^+ - p_1^+)$, respectively, for $\mathbb{C} = 0$. Thus, all three $x^{\hat{+}}$-ordered amplitudes are invariant under T_{12} regardless of the $\mathbb{C}$ values as they should be.

Now, applying the longitudinal boost T_3 to the three time-ordered amplitudes, we note that the operator $K^3 = M_{\hat{+}\hat{-}}$ changes its characteristic from dynamic for $\mathbb{C} \neq 0$ to kinematic in the light front ($\mathbb{C} = 0$) as shown in Table I, which summarizes the set of kinematic and dynamic generators depending on the interpolation angle. We mentioned this point in Sec. II and provided its elaborate discussion in Refs. [20,21]. In applying $T_3 = e^{-iK_3\beta^3}$, we thus distinguish the values of $\mathbb{C}$ between $\mathbb{C} \neq 0$ and $\mathbb{C} = 0$. We first consider the $\mathbb{C} \neq 0$ case and later compare the results in this case with the LFD ($\mathbb{C} = 0$) results.

For the kinematics of our two-body scattering process analogous to $e\mu \to e\mu$, we choose the scattering plane as the $x - z$ plane and the directions of the initial two particles as the parallel/antiparallel to the z axis such that $\mathbf{p}_{1\perp} = \mathbf{p}_{2\perp} = 0$ as shown in Fig. 1. In the center-of-momentum frame (CMF), we have $p_1^z = -p_2^z \equiv p$, $\epsilon_1 \equiv p_1^0 = p_3^0 = \sqrt{p^2 + m_1^2}$, $\epsilon_2 \equiv p_2^0 = p_4^0 = \sqrt{p^2 + m_2^2}$, and $M \equiv \epsilon_1 + \epsilon_2$, where we denote the total energy in the CMF as M for the convenience in the later discussion. We should note that the invariant Mandelstam variable $s = (p_1 + p_2)^2$ is given by M^2. The final 4-momenta p_3 and p_4 of the particles that are going back to back at angle θ in the CMF are depicted in Fig. 1. Correspondingly, the 4-momenta of the initial and final particles in the CMF are given by

$$p_1 = (\epsilon_1, 0, 0, p), \tag{89a}$$

$$p_2 = (\epsilon_2, 0, 0, -p), \tag{89b}$$

$$p_3 = (\epsilon_1, p\sin\theta, 0, p\cos\theta), \tag{89c}$$

$$p_4 = (\epsilon_2, -p\sin\theta, 0, -p\cos\theta). \tag{89d}$$

To discuss the longitudinal boost (T_3) effect on time-ordered scattering amplitudes, let us now boost the whole system to the total momentum P^z. From the Lorentz transformation for a composite free particle system, we know that the total energy in the new frame is $E = \sqrt{(P^z)^2 + M^2}$. The Lorentz transformation for each p_i $(i = 1, 2, 3, 4)$ can then be described in terms of $\gamma = E/M$ and $\gamma\beta = P^z/M$:

$$p'^0_i = \gamma p_i^0 + \gamma\beta p_i^z \tag{90a}$$

$$p'^z_i = \gamma p_i^z + \gamma\beta p_i^0 \tag{90b}$$

$$\mathbf{p}'^\perp_i = \mathbf{p}^\perp_i. \tag{90c}$$

The boosted 4-momentum transfer can therefore be written as

$$q'^x = p'^x_1 - p'^x_3 = -p\sin\theta, \tag{91a}$$

$$q'^y = p'^y_1 - p'^y_3 = 0, \tag{91b}$$

$$q'^z = p'^z_1 - p'^z_3 = \frac{E}{M}p(1 - \cos\theta), \tag{91c}$$

$$q'^0 = p'^0_1 - p'^0_3 = \frac{P^z}{M}p(1 - \cos\theta), \tag{91d}$$

where M and E are functions of m_1, m_2, p, and P^z. We can use these 4-momentum components given by Eq. (91) and apply Eq. (6) to form $q'^{\hat{\mu}}$ and $q'_{\hat{\mu}}$ for any interpolation angle. Equation (90) can also be used together with Eqs. (6) and (87) to express all the components of the boosted 4-momenta. Computing $p'_{24} \cdot p'_{13}$ and plugging it with other factors such as $p'^{\hat{+}}_{24}\, p'^{\hat{+}}_{13}$ and $q'_{\hat{\mu}}$ into Eq. (71) and subsequently Eq. (86), we get the interpolating time-ordered amplitudes $\mathcal{M}'^{(j)}$ in a boosted frame. In the CMF, all of these amplitudes are then given by functions of each particle's initial momentum $p(-p)$, individual particle's rest mass m_1 and m_2, scattering angle θ, the total momentum P^z, and the interpolation angle δ. For given values of m_1, m_2, p, and θ, the $x^{\hat{+}}$-ordered amplitudes are dependent on the frame (P^z) and the interpolation angle (δ or $\mathbb{C}$).

To exhibit this feature quantitatively, we choose $m_1 = 1$, $m_2 = 2$, and $p = 3$, in the same energy unit (i.e., m_2 and p scaled by m_1), and $\theta = \pi/3$. For simplicity, we also take the charge e to be 1 unit in our calculation. In Fig. 2, we plot $\mathcal{M}^{(a)}$, $\mathcal{M}^{(b)}$, $\mathcal{M}^{(c)}$ as well as the sum of all three amplitudes $\mathcal{M}^{(\mathrm{tot})}$ as functions of both the interpolation angle δ and the total momentum P^z to reflect not only the interpolation angle dependence but also the frame dependence. The total amplitude $\mathcal{M}^{(\mathrm{tot})}$ shown in Fig. 2 is both frame independent and interpolation angle independent as it should be.

The detailed structures of these three time-ordered diagrams are very interesting. Just like in the ϕ^3 toy model theory studied in Ref. [21], the $P^z > 0$ region is smooth for all three amplitudes, while a J-shaped correlation curve exists in the $P^z < 0$ region, which we plotted as the red solid line in Fig. 2. This is the curve that starts out in the center-of-mass frame ($P^z = 0$) in the $\delta = 0$ limit but maintains the same value of the amplitude throughout the whole range of the interpolation angle. The values maintained by these curves can be found for arbitrary m_1, m_2, p, and θ and are given by

$$\mathcal{M}^{(a)} = \mathcal{M}^{(b)} = -\frac{\cot^2\frac{\theta}{2}}{2}, \tag{92a}$$

$$\mathcal{M}^{(c)} = -\frac{\epsilon_1\epsilon_2}{p^2\sin^2\frac{\theta}{2}}. \tag{92b}$$

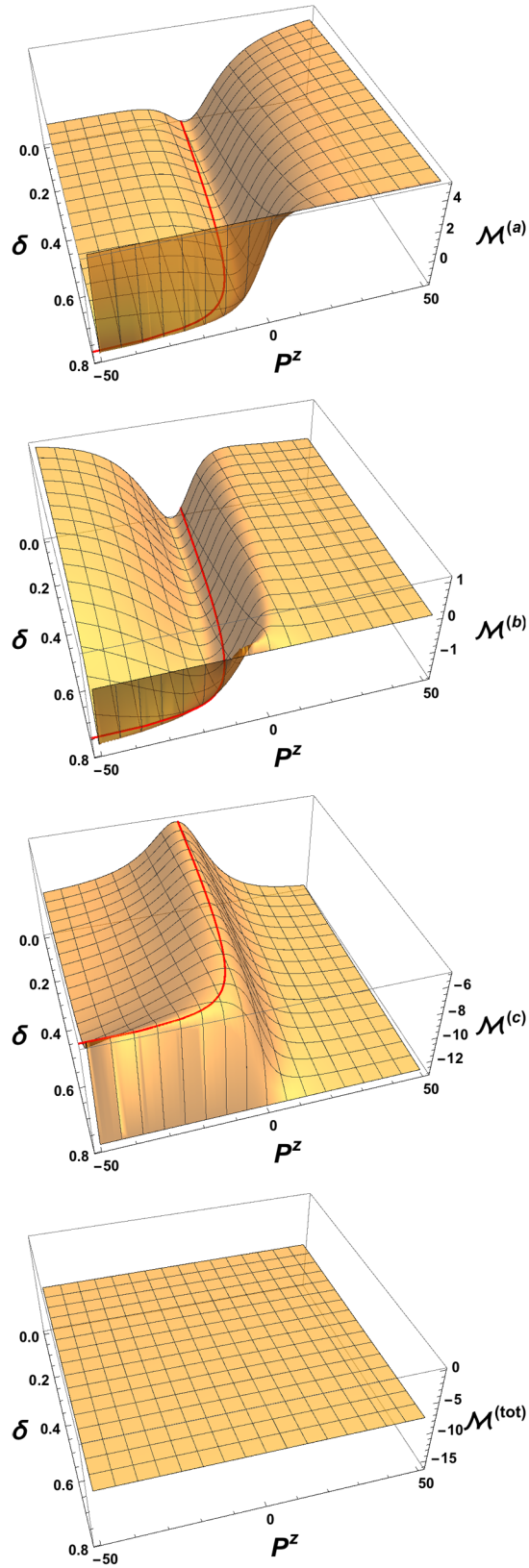

FIG. 2 (color online). Time-ordered amplitudes $\mathcal{M}^{(a)}$, $\mathcal{M}^{(b)}$, and $\mathcal{M}^{(c)}$ for $m_1 = 1, m_2 = 2, p = 3$, and $\theta = \pi/3$ and their sum $\mathcal{M}^{(\mathrm{tot})}$.

Again, $\epsilon_i = \sqrt{q^2 + m_i^2}$ $(i = 1, 2)$, and the charge e in Eq. (86) is taken as 1 unit.

In Fig. 3, we plot the profiles of $\mathcal{M}^{(a)}$, $\mathcal{M}^{(b)}$, and $\mathcal{M}^{(c)}$ in the IFD ($\mathbb{C} = 1$ or $\delta = 0$) for the given values of m_1, m_2, p, and θ and depict the starting point of the J curve corresponding to the values of $\mathcal{M}^{(a)}$, $\mathcal{M}^{(b)}$, and $\mathcal{M}^{(c)}$ at $P^z = 0$ given by Eqs. (92). The maxima for $\mathcal{M}^{(a)}$ and $\mathcal{M}^{(b)}$ stay in the $P^z > 0$ and $P^z < 0$ regions, respectively, but as the scattering angle θ approaches 0, the maximum for $\mathcal{M}^{(a)}$ and $\mathcal{M}^{(b)}$ will move toward $P^z = 0$. As the J curve does not track the maximum or the minimum in $\mathcal{M}^{(a)}$ and $\mathcal{M}^{(b)}$, we note that the J curve does not track the maximum of the surface $M^{(c)}$ either.

It is interesting to note that the J curve itself does not change with the scattering angle θ. In fact, we find that it follows exactly the same formula as the one we found in the ϕ^3 theory [21],

$$\frac{P^z}{M} = -\sqrt{\frac{(1-\mathbb{C})}{2\mathbb{C}}}, \tag{93}$$

where M^2 is identical to the invariant Mandelstam variable $s = (p_1 + p_2)^2$, i.e., $M = \sqrt{s}$. We note that the J curve is "universal" in the sense that it does not depend on the specific kinematics like the scattering angle or particle masses but scales with $\sqrt{s}$.

If we follow this J curve plotted as the red solid line in Fig. 2, we see that, as $\mathbb{C} \to 0$ or $\delta \to \pi/4$, it is pushed to $P^z \to -\infty$, and the constant values given by Eq. (92) are maintained throughout the curve. On the other hand, the x^+-ordered light-front amplitudes are invariant under the longitudinal boost $T_3 = e^{-iK_3\beta^3}$, and thus each of $\mathcal{M}^{(a)}$, $\mathcal{M}^{(b)}$, and $\mathcal{M}^{(c)}$ shows up individually as a constant independent of P^z along the $\delta = \pi/4$ or $\mathbb{C} = 0$ line in Fig. 2. Thus, the values of $\mathcal{M}^{(a)}$, $\mathcal{M}^{(b)}$, and $\mathcal{M}^{(c)}$ in the limit $\mathbb{C} \to 0$ following the J curve are different from those in the LFD, i.e., at the exact $\mathbb{C} = 0$. This brings up our discussion in the last subsection, Sec. IV C, about the issue of whether the LFD results with the exact $\mathbb{C} = 0$ can be reproduced by taking the limit $\mathbb{C} \to 0$. Because all the plus components of the particle momenta vanish in the limit $P^z \to -\infty$, we should look closely at the kinematic situation $p_1^+ = p_3^+ = q^+ = 0$, the discussion of which we have postponed until now in Sec. IV C.

Since the details of each contribution depend on the values of $\mathbb{C}$ and P^z, the results are in general dependent on the order of taking the limits to $\mathbb{C} \to 0$ and $P^z \to -\infty$. In particular, if $\mathbb{C} = 0$ is taken first, then the results must be independent of the P^z values due to the longitudinal boost invariance in the LFD as discussed before, and the result at $P^z = -\infty$ is identical to that for any other P^z value. However, if we take $P^z \to -\infty$ first and consider $\mathbb{C} \to 0$, then we should first examine the $\mathbb{C} \neq 0$ results in the $P^z \to -\infty$ limit with great care. We begin with the

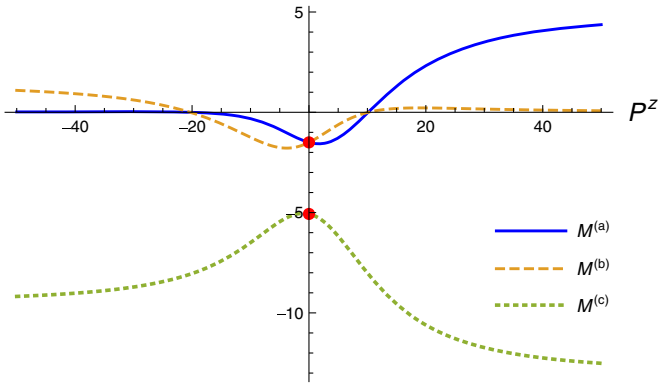

FIG. 3 (color online). Time-ordered amplitudes $\mathcal{M}^{(a)}$, $\mathcal{M}^{(b)}$, and $\mathcal{M}^{(c)}$ as a function of the total momentum P^z at the instant form limit ($\delta = 0$). The red dots on the $P^z = 0$ axis denote the starting position of the J curves on each surface.

discussion on the $\mathbb{C} = 1$ (i.e., the IFD) results and vary the interpolation angle from $\delta = 0$ to $\delta \to \pi/4$.

As shown in Figs. 2 and 3, each of the time-ordered amplitudes $\mathcal{M}^{(a)}$, $\mathcal{M}^{(b)}$, and $\mathcal{M}^{(c)}$ at $\mathbb{C} = 1(\delta = 0)$ is not symmetric under the reflection of $P^z \to -P^z$. Although the IFD results coincide with the LFD results as $P^z \to \infty$, they do not agree in the limit $P^z \to -\infty$ as shown in Fig. 2. Thus, the prevailing notion of the equivalence between the IFD and LFD in the IMF should be taken with a great caution since it works for the limit of $P_z \to \infty$ but not in the limit $P_z \to -\infty$. We have already discussed the treachery in taking the limit $P_z \to -\infty$ even for the amplitudes with the reflection symmetry under $P^z \leftrightarrow -P^z$ in the IFD such as the scalar annihilation process analogous to QED $e^+e^- \to \mu^+\mu^-$ in our previous work [21]. The present analysis of the sQED scattering process analogous to QED $e\mu \to e\mu$ provides a clear example of breaking the reflection symmetry under $P^z \leftrightarrow -P^z$ in the IFD and fortifies the clarification of the confusion in the folklore of the equivalence between the IMF and the LFD. As we vary the interpolation angle from $\delta = 0$ and approach to $\delta = \pi/4$, this broken reflection symmetry under $P^z \leftrightarrow -P^z$ persists while the LFD results are symmetric under $P^z \leftrightarrow -P^z$ due to the longitudinal boost invariance discussed previously. The J-curve correlation between P^z and $\mathbb{C}$ given by Eq. (93) provides a simultaneous limit of $P^z \sim -1/\mathbb{C}^{1/2} \to -\infty$ as $\mathbb{C} \to 0$, and the corresponding results of $\mathcal{M}^{(a)}$, $\mathcal{M}^{(b)}$, and $\mathcal{M}^{(c)}$ are uniquely given by Eqs. (92a) and (92b). As mentioned earlier, the numerical values along the J curve plotted as the red solid line in Fig. 2 are identical all the way to the $P^z \to -\infty$ limit, and thus the clear distinction is manifest between the results in the $\mathbb{C} \to 0$ limit with the J-curve correlation and the LFD results with the exact $\mathbb{C} = 0$. Since the J curve exists only for $P^z < 0$, it is also self-evident that the broken reflection symmetry under $P^z \leftrightarrow -P^z$ still persists for the correlated limit of $P^z \sim -1/\mathbb{C}^{1/2} \to -\infty$ and the results obtained in this limit must be different from the LFD results. Therefore, the limit $P^z \to -\infty$ is treacherous and requires great caution in taking the light-front limit from $\mathbb{C} \neq 0$. As it must be, however, the sum of all time-ordered amplitudes $\mathcal{M}^{(\mathrm{tot})} = \mathcal{M}^{(a)} + \mathcal{M}^{(b)} + \mathcal{M}^{(c)}$ is completely independent of $\mathbb{C}$ and P^z. The total amplitude $\mathcal{M}^{(\mathrm{tot})}$ is of course identical regardless of whether $\mathbb{C}$ is exactly zero or not, however the limit $P^z \to -\infty$ is taken.

Finally, we also calculated the time-ordered scattering amplitudes discussed in this section for the scalar ϕ^3 theory that was used in our previous work [21] and summarized the results in Appendix D for a comparison with the sQED results. For completeness in comparing the results between the ϕ^3 theory and sQED, the time-ordered annihilation amplitudes for sQED are summarized also in Appendix E.

VI. SUMMARY AND CONCLUSION

In this work, we extended the interpolating scattering amplitudes introduced for the scalar field theory [21] to the sQED theory to discuss the electromagnetic gauge degree of freedom interpolated between the IFD and the LFD. We developed the electromagnetic gauge field propagator interpolated between the IFD and the LFD and found that the light-front gauge $A^+ = 0$ in the LFD is naturally linked to the Coulomb gauge $\nabla \cdot \mathbf{A} = 0$ in the IFD. We identified the dynamical degrees of freedom for the electromagnetic gauge fields as the transverse photon fields and clarified the equivalence between the contribution of the instantaneous interaction and the contribution from the longitudinal polarization of the virtual photon.

Our results for the gauge propagator and time-ordered diagrams clarified whether one should choose the two-term form [8] or the three-term form [25–27] for the gauge propagator in the LFD. Our transverse photon propagator in the LFD assumes the three-term form, but the third term cancels the instantaneous interaction contribution. Thus, one can use the two-term form of the gauge propagator for effective calculation of amplitudes if one also omits the instantaneous interaction from the Hamiltonian. But if one wants to show equivalence to the covariant theory, all three terms should be kept because the instantaneous interaction is a natural result of the decomposition of Feynman diagrams, and the third term in the propagator is necessary for the total amplitudes to be covariant. We also see that the photon propagator was derived according to the generalized gauge that links the Coulomb gauge to light-front gauge, and thus the three-term form appears appropriate in order to be consistent with the appropriate gauge.

Using the interpolating photon propagator, we computed the lowest-order scattering process such as an analog of the well-known QED process $e\mu \to e\mu$ in sQED and analyzed the three corresponding $x^{\hat{+}}$-ordered diagrams, two of which are associated with the transverse propagating photon and one of which is associated with the instantaneous

interaction. We analyzed both the frame and interpolation angle dependence of each $x^{\hat{+}}$-ordered diagram including the instantaneous interaction, varying the total momentum P^z of the system and the interpolation angle parameter $\mathbb{C} = \cos 2\delta$. Our analysis provided a clear example of breaking the reflection symmetry under $P^z \leftrightarrow -P^z$ in the IFD and clarified the confusion in the folklore of the equivalence between the IMF and the LFD. As we vary the interpolation angle from $\delta = 0$ ($\mathbb{C} = 1$) and approach to $\delta = \pi/4$ ($\mathbb{C} = 0$), this broken reflection symmetry under $P^z \leftrightarrow -P^z$ persists while the LFD results are symmetric under $P^z \leftrightarrow -P^z$ due to the longitudinal boost invariance. Moreover, the universal correlation between P^z and $\mathbb{C}$ given by Eq. (93) that was coined as the J curve in our previous work [21] is intact in each of these $x^{\hat{+}}$-ordered diagrams as plotted by the red solid line in Fig. 2. The J curve starts out from the center-of-mass frame in the instant form and goes to $P^z = -\infty$ as it approaches to the light-front limit. This correlation is independent of the specific kinematics of the scattering process and manifests the difference in the results between the light-front limit and the exact light-front (LFD). Since the J curve exists only for $P^z < 0$, it is also self-evident that the broken reflection symmetry under $P^z \leftrightarrow -P^z$ still persists for the correlated limit of $P^z \sim -1/\mathbb{C}^{1/2} \to -\infty$ and the results obtained in this limit must be different from the LFD results. The J curve not only provides a representative characterization of how the $x^{\hat{+}}$-ordered amplitudes change from the IFD to the LFD but also gives rise to the issue of zero modes at $P^z = -\infty$ since all the plus momenta of particles vanish in this limit. The limit $P^z \to -\infty$ is thus treacherous and requires a great caution in taking the light-front limit from $\mathbb{C} \neq 0$. The sum of all $x^{\hat{+}}$-ordered amplitudes is, however, completely independent of $\mathbb{C}$ and P^z, and its full manifest Poincaré invariance provides a useful guidance in handling the treacherous zero-mode issue.

ACKNOWLEDGMENTS

This work was supported by the U.S. Department of Energy (Grant No. DE-FG02-03ER41260) and the FAPESP-NC (Grant No. NCSU RADAR 2014-0717).

APPENDIX A: DERIVATION OF PHOTON POLARIZATION VECTORS

We use the explicit 4-vector representation of **K** and **J** operators given by

$$K_1 = \begin{pmatrix} 0 & i & 0 & 0 \\ i & 0 & 0 & 0 \\ 0 & 0 & 0 & 0 \\ 0 & 0 & 0 & 0 \end{pmatrix}, \quad K_2 = \begin{pmatrix} 0 & 0 & i & 0 \\ 0 & 0 & 0 & 0 \\ i & 0 & 0 & 0 \\ 0 & 0 & 0 & 0 \end{pmatrix}, \quad K_3 = \begin{pmatrix} 0 & 0 & 0 & i \\ 0 & 0 & 0 & 0 \\ 0 & 0 & 0 & 0 \\ i & 0 & 0 & 0 \end{pmatrix},$$

$$J_1 = \begin{pmatrix} 0 & 0 & 0 & 0 \\ 0 & 0 & 0 & 0 \\ 0 & 0 & 0 & -i \\ 0 & 0 & i & 0 \end{pmatrix}, \quad J_2 = \begin{pmatrix} 0 & 0 & 0 & 0 \\ 0 & 0 & 0 & i \\ 0 & 0 & 0 & 0 \\ 0 & -i & 0 & 0 \end{pmatrix}, \quad J_3 = \begin{pmatrix} 0 & 0 & 0 & 0 \\ 0 & 0 & -i & 0 \\ 0 & i & 0 & 0 \\ 0 & 0 & 0 & 0 \end{pmatrix}. \tag{A1}$$

Upon the application of T transformation given by Eq. (15) with the above 4-vector representation for operators **K** and **J**, we find the polarization vectors:

$$\epsilon_{\hat{\mu}}(P,+) = -\begin{bmatrix} \frac{\sin\delta}{\sqrt{2}}\left(\frac{\beta_1 \sin\alpha}{\alpha} - \frac{i\beta_2 \sin\alpha}{\alpha}\right) \\ \frac{\mathbb{C}}{\sqrt{2}}\left(\frac{\beta_2^2 + \beta_1^2 \cos\alpha}{\alpha^2} + \frac{i\beta_1\beta_2(-1+\cos\alpha)}{\alpha^2}\right) \\ \frac{\mathbb{C}}{\sqrt{2}}\left(\frac{\beta_1\beta_2(-1+\cos\alpha)}{\alpha^2} + \frac{i(\beta_1^2 + \beta_2^2\cos\alpha)}{\alpha^2}\right) \\ -\frac{\cos\delta}{\sqrt{2}}\left(\frac{\beta_1 \sin\alpha}{\alpha} + \frac{i\beta_2 \sin\alpha}{\alpha}\right) \end{bmatrix}, \quad \epsilon_{\hat{\mu}}(P,-) = \begin{bmatrix} \frac{\sin\delta}{\sqrt{2}}\left(\frac{\beta_1 \sin\alpha}{\alpha} + \frac{i\beta_2 \sin\alpha}{\alpha}\right) \\ \frac{\mathbb{C}}{\sqrt{2}}\left(\frac{\beta_2^2 + \beta_1^2 \cos\alpha}{\alpha^2} - \frac{i\beta_1\beta_2(-1+\cos\alpha)}{\alpha^2}\right) \\ \frac{\mathbb{C}}{\sqrt{2}}\left(\frac{\beta_1\beta_2(-1+\cos\alpha)}{\alpha^2} - \frac{i(\beta_1^2 + \beta_2^2\cos\alpha)}{\alpha^2}\right) \\ -\frac{\cos\delta}{\sqrt{2}}\left(\frac{\beta_1 \sin\alpha}{\alpha} - \frac{i\beta_2 \sin\alpha}{\alpha}\right) \end{bmatrix}, \tag{A2}$$

$$\epsilon_{\hat{\mu}}(P,0) = \begin{bmatrix} \dfrac{\cos\delta(\sin\delta\cosh\beta_3 + \cos\delta\sinh\beta_3) - \sin\delta\cos\alpha(\cos\delta\cosh\beta_3 + \sin\delta\sinh\beta_3)}{\mathbb{C}} \\ \dfrac{\beta_1\sin\alpha(\sin\delta\cosh\beta_3 + \cos\delta\sinh\beta_3)}{\alpha} \\ \dfrac{\beta_2\sin\alpha(\sin\delta\cosh\beta_3 + \cos\delta\sinh\beta_3)}{\alpha} \\ \dfrac{\cos\delta\cos\alpha(\cos\delta\cosh\beta_3 + \sin\delta\sinh\beta_3) - \sin\delta(\sin\delta\cosh\beta_3 + \cos\delta\sinh\beta_3)}{\mathbb{C}} \end{bmatrix}. \tag{A3}$$

Using the relations listed in Eqs. (18) and (19) and multiplying the transverse polarization vectors $\epsilon_{\hat{\mu}}(P,\pm)$ with the phase factor $\frac{P^1 \mp P^2}{|\mathbf{P}_\perp|}$ to simplify, we arrive at the following polarization vectors for the 4-momentum P^μ:

$$\epsilon_{\hat{\mu}}(P,+) = -\frac{1}{\sqrt{2}\mathbb{P}}\left(\sin\delta|\mathbf{P}_\perp|, \frac{P^1P_{\hat{-}} - iP^2\mathbb{P}}{|\mathbf{P}_\perp|}, \frac{P^2P_{\hat{-}} + iP^1\mathbb{P}}{|\mathbf{P}_\perp|}, -\cos\delta|\mathbf{P}_\perp|\right), \tag{A4}$$

$$\epsilon_{\hat{\mu}}(P,-) = \frac{1}{\sqrt{2}\mathbb{P}}\left(\sin\delta|\mathbf{P}_\perp|, \frac{P^1P_{\hat{-}} + iP^2\mathbb{P}}{|\mathbf{P}_\perp|}, \frac{P^2P_{\hat{-}} - iP^1\mathbb{P}}{|\mathbf{P}_\perp|}, -\cos\delta|\mathbf{P}_\perp|\right), \tag{A5}$$

$$\epsilon_{\hat{\mu}}(P,0) = \frac{1}{M\mathbb{P}}\left(\frac{\mathbb{P}^2\cos\delta - P_{\hat{-}}P^{\hat{+}}\sin\delta}{\mathbb{C}}, P^1P^{\hat{+}}, P^2P^{\hat{+}}, \frac{P^{\hat{+}}P_{\hat{-}}\cos\delta - \mathbb{P}^2\sin\delta}{\mathbb{C}}\right). \tag{A6}$$

The polarization vectors listed above are written in the form $\epsilon_{\hat{\mu}}(P,\lambda) = (\epsilon^0, \epsilon^1, \epsilon^2, \epsilon^3)$. We then change the basis to $(\epsilon_{\hat{+}}, \epsilon_1, \epsilon_2, \epsilon_{\hat{-}})$ using the relations listed in Eq. (7). Finally, we obtain the polarization vectors given by Eq. (22),

$$\epsilon_{\hat{\mu}}(P,+) = -\frac{1}{\sqrt{2}\mathbb{P}}\left(\mathbb{S}|\mathbf{P}_\perp|, \frac{P_1P_{\hat{-}} - iP_2\mathbb{P}}{|\mathbf{P}_\perp|}, \frac{P_2P_{\hat{-}} + iP_1\mathbb{P}}{|\mathbf{P}_\perp|}, -\mathbb{C}|\mathbf{P}_\perp|\right), \tag{A7a}$$

$$\epsilon_{\hat{\mu}}(P,-) = \frac{1}{\sqrt{2}\mathbb{P}}\left(\mathbb{S}|\mathbf{P}_\perp|, \frac{P_1P_{\hat{-}} + iP_2\mathbb{P}}{|\mathbf{P}_\perp|}, \frac{P_2P_{\hat{-}} - iP_1\mathbb{P}}{|\mathbf{P}_\perp|}, -\mathbb{C}|\mathbf{P}_\perp|\right), \tag{A7b}$$

$$\epsilon_{\hat{\mu}}(P,0) = \frac{P^{\hat{+}}}{M\mathbb{P}}\left(P_{\hat{+}} - \frac{M^2}{P^{\hat{+}}}, P_1, P_2, P_{\hat{-}}\right), \tag{A7c}$$

where the relation $\mathbb{P}^2 = (P^{\hat{+}})^2 - M^2\mathbb{C}$ is used to derive the first component of $\epsilon_{\hat{\mu}}(P,0)$.

APPENDIX B: $\mathcal{T}_{\hat{\mu}\hat{\nu}}$ AND $\mathcal{L}_{\hat{\mu}\hat{\nu}}$ DERIVED DIRECTLY FROM THE INTERPOLATING POLARIZATION VECTORS

In this Appendix, we derive the numerator of the photon propagator directly from the polarization vectors listed in Eqs. (22) and (A7).

We evaluate the relevant matrix elements. With the 4-momentum $P = q$ for the virtual photon, these are, for $\lambda = +1$,

$$\epsilon^*_{\hat{+}}(q,\lambda=+)\epsilon_{\hat{+}}(q,\lambda=+) = \frac{\mathbb{S}^2|\mathbf{q}_\perp|^2}{2\mathbb{Q}^2}, \tag{B1}$$

$$\epsilon^*_{\hat{+}}(q,\lambda=+)\epsilon_1(q,\lambda=+) = \frac{\mathbb{S}(q_{\hat{-}}q_1 - iq_2\mathbb{Q})}{2\mathbb{Q}^2}, \tag{B2}$$

$$\epsilon^*_{\hat{+}}(q,\lambda=+)\epsilon_2(q,\lambda=+) = \frac{\mathbb{S}(q_{\hat{-}}q_2 + iq_1\mathbb{Q})}{2\mathbb{Q}^2}, \tag{B3}$$

$$\epsilon^*_{\hat{+}}(q,\lambda=+)\epsilon_{\hat{-}}(q,\lambda=+) = -\frac{\mathbb{C}\mathbb{S}|\mathbf{q}_\perp|^2}{2\mathbb{Q}^2}, \tag{B4}$$

$$\epsilon^*_{\hat{-}}(q,\lambda=+)\epsilon_{\hat{+}}(q,\lambda=+) = -\frac{\mathbb{C}\mathbb{S}|\mathbf{q}_\perp|^2}{2\mathbb{Q}^2}, \tag{B5}$$

$$\epsilon^*_{\hat{-}}(q,\lambda=+)\epsilon_1(q,\lambda=+) = -\frac{\mathbb{C}(q_{\hat{-}}q_1 - iq_2\mathbb{Q})}{2\mathbb{Q}^2}, \tag{B6}$$

$$\epsilon^*_{\hat{-}}(q,\lambda=+)\epsilon_2(q,\lambda=+) = -\frac{\mathbb{C}(q_{\hat{-}}q_2 + iq_1\mathbb{Q})}{2\mathbb{Q}^2}, \tag{B7}$$

$$\epsilon^*_{\hat{-}}(q,\lambda=+)\epsilon_{\hat{-}}(q,\lambda=+) = \frac{\mathbb{C}^2|\mathbf{q}_\perp|^2}{2\mathbb{Q}^2}, \tag{B8}$$

$$\epsilon_1^*(q,\lambda=+)\epsilon_{\hat{+}}(q,\lambda=+)=\frac{\mathbb{S}(q_{\hat{-}}q_1+iq_2\mathbb{Q})}{2\mathbb{Q}^2}, \tag{B9}$$

$$\epsilon_1^*(q,\lambda=+)\epsilon_1(q,\lambda=+)=\frac{q_{\hat{-}}^2q_1^2+q_2^2\mathbb{Q}^2}{2|\mathbf{q}_\perp|^2\mathbb{Q}^2}, \tag{B10}$$

$$\epsilon_1^*(q,\lambda=+)\epsilon_2(q,\lambda=+)=\frac{-\mathbb{C}q_1q_2+iq_{\hat{-}}\mathbb{Q}}{2\mathbb{Q}^2}, \tag{B11}$$

$$\epsilon_1^*(q,\lambda=+)\epsilon_{\hat{-}}(q,\lambda=+)=\frac{-\mathbb{C}(q_{\hat{-}}q_1+iq_2\mathbb{Q})}{2\mathbb{Q}^2}, \tag{B12}$$

$$\epsilon_2^*(q,\lambda=+)\epsilon_{\hat{+}}(q,\lambda=+)=\frac{\mathbb{S}(q_{\hat{-}}q_2-iq_1\mathbb{Q})}{2\mathbb{Q}^2}, \tag{B13}$$

$$\epsilon_2^*(q,\lambda=+)\epsilon_1(q,\lambda=+)=\frac{-\mathbb{C}q_1q_2-iq_{\hat{-}}\mathbb{Q}}{2\mathbb{Q}^2}, \tag{B14}$$

$$\epsilon_2^*(q,\lambda=+)\epsilon_2(q,\lambda=+)=\frac{q_{\hat{-}}^2q_2^2+q_1^2\mathbb{Q}^2}{2|\mathbf{q}_\perp|^2\mathbb{Q}^2}, \tag{B15}$$

$$\epsilon_2^*(q,\lambda=+)\epsilon_{\hat{-}}(q,\lambda=+)=\frac{-\mathbb{C}(q_{\hat{-}}q_2-iq_1\mathbb{Q})}{2\mathbb{Q}^2}, \tag{B16}$$

and for $\lambda=-1$,

$$\epsilon_{\hat{+}}^*(q,\lambda=-)\epsilon_{\hat{+}}(q,\lambda=-)=\frac{\mathbb{S}^2|\mathbf{q}_\perp|^2}{2\mathbb{Q}^2}, \tag{B17}$$

$$\epsilon_{\hat{+}}^*(q,\lambda=-)\epsilon_1(q,\lambda=-)=\frac{\mathbb{S}(q_{\hat{-}}q_1+iq_2\mathbb{Q})}{2\mathbb{Q}^2}, \tag{B18}$$

$$\epsilon_{\hat{+}}^*(q,\lambda=-)\epsilon_2(q,\lambda=-)=\frac{\mathbb{S}(q_{\hat{-}}q_2-iq_1\mathbb{Q})}{2\mathbb{Q}^2}, \tag{B19}$$

$$\epsilon_{\hat{+}}^*(q,\lambda=-)\epsilon_{\hat{-}}(q,\lambda=-)=-\frac{\mathbb{C}\mathbb{S}|\mathbf{q}_\perp|^2}{2\mathbb{Q}^2}, \tag{B20}$$

$$\epsilon_{\hat{-}}^*(q,\lambda=-)\epsilon_{\hat{+}}(q,\lambda=-)=-\frac{\mathbb{C}\mathbb{S}|\mathbf{q}_\perp|^2}{2\mathbb{Q}^2}, \tag{B21}$$

$$\epsilon_{\hat{-}}^*(q,\lambda=-)\epsilon_1(q,\lambda=-)=-\frac{\mathbb{C}(q_{\hat{-}}q_1+iq_2\mathbb{Q})}{2\mathbb{Q}^2}, \tag{B22}$$

$$\epsilon_{\hat{-}}^*(q,\lambda=-)\epsilon_2(q,\lambda=-)=-\frac{\mathbb{C}(q_{\hat{-}}q_2-iq_1\mathbb{Q})}{2\mathbb{Q}^2}, \tag{B23}$$

$$\epsilon_{\hat{-}}^*(q,\lambda=-)\epsilon_{\hat{-}}(q,\lambda=-)=\frac{\mathbb{C}^2|\mathbf{q}_\perp|^2}{2\mathbb{Q}^2}, \tag{B24}$$

$$\epsilon_1^*(q,\lambda=-)\epsilon_{\hat{+}}(q,\lambda=-)=\frac{\mathbb{S}(q_{\hat{-}}q_1-iq_2\mathbb{Q})}{2\mathbb{Q}^2}, \tag{B25}$$

$$\epsilon_1^*(q,\lambda=-)\epsilon_1(q,\lambda=-)=\frac{q_{\hat{-}}^2q_1^2+q_2^2\mathbb{Q}^2}{2|\mathbf{q}_\perp|^2\mathbb{Q}^2}, \tag{B26}$$

$$\epsilon_1^*(q,\lambda=-)\epsilon_2(q,\lambda=-)=\frac{-\mathbb{C}q_1q_2-iq_{\hat{-}}\mathbb{Q}}{2\mathbb{Q}^2}, \tag{B27}$$

$$\epsilon_1^*(q,\lambda=-)\epsilon_{\hat{-}}(q,\lambda=-)=\frac{-\mathbb{C}(q_{\hat{-}}q_1-iq_2\mathbb{Q})}{2\mathbb{Q}^2}, \tag{B28}$$

$$\epsilon_2^*(q,\lambda=-)\epsilon_{\hat{+}}(q,\lambda=-)=\frac{\mathbb{S}(q_{\hat{-}}q_2+iq_1\mathbb{Q})}{2\mathbb{Q}^2}, \tag{B29}$$

$$\epsilon_2^*(q,\lambda=-)\epsilon_1(q,\lambda=-)=\frac{-\mathbb{C}q_1q_2+iq_{\hat{-}}\mathbb{Q}}{2\mathbb{Q}^2}, \tag{B30}$$

$$\epsilon_2^*(q,\lambda=-)\epsilon_2(q,\lambda=-)=\frac{q_{\hat{-}}^2q_2^2+q_1^2\mathbb{Q}^2}{2|\mathbf{q}_\perp|^2\mathbb{Q}^2}, \tag{B31}$$

$$\epsilon_2^*(q,\lambda=-)\epsilon_{\hat{-}}(q,\lambda=-)=\frac{-\mathbb{C}(q_{\hat{-}}q_2+iq_1\mathbb{Q})}{2\mathbb{Q}^2}, \tag{B32}$$

where $\mathbb{Q}\equiv\sqrt{q_{\hat{-}}^2+\mathbf{q}_\perp^2\mathbb{C}}$.

By defining $\mathcal{T}_{\hat{\mu}\hat{\nu}}=\sum_{\lambda=+,-}\epsilon_{\hat{\mu}}^*(q,\lambda)\epsilon_{\hat{\nu}}(q,\lambda)$, we obtain the following matrix form:

$$\mathcal{T}_{\hat{\mu}\hat{\nu}}=\frac{1}{\mathbb{Q}^2}\begin{pmatrix}\mathbb{S}^2|\mathbf{q}_\perp|^2 & \mathbb{S}q_{\hat{-}}q_1 & \mathbb{S}q_{\hat{-}}q_2 & -\mathbb{C}\mathbb{S}|\mathbf{q}_\perp|^2\\ \mathbb{S}q_{\hat{-}}q_1 & q_{\hat{-}}^2+\mathbb{C}q_2^2 & -\mathbb{C}q_1q_2 & -\mathbb{C}q_{\hat{-}}q_1\\ \mathbb{S}q_{\hat{-}}q_2 & -\mathbb{C}q_1q_2 & q_{\hat{-}}^2+\mathbb{C}q_1^2 & -\mathbb{C}q_{\hat{-}}q_2\\ -\mathbb{C}\mathbb{S}|\mathbf{q}_\perp|^2 & -\mathbb{C}q_{\hat{-}}q_1 & -\mathbb{C}q_{\hat{-}}q_2 & \mathbb{C}^2|\mathbf{q}_\perp|^2\end{pmatrix}. \tag{B33}$$

This can be written in general as

$$\mathcal{T}_{\hat{\mu}\hat{\nu}}=-g_{\hat{\mu}\hat{\nu}}+X(q_{\hat{\mu}}n_{\hat{\nu}}+n_{\hat{\mu}}q_{\hat{\nu}})+Yn_{\hat{\mu}}n_{\hat{\nu}}+Zq_{\hat{\mu}}q_{\hat{\nu}}, \tag{B34}$$

where the coefficients X, Y, and Z can be fixed by comparing this equation with the explicit matrix form given by Eq. (B33). We find

$$X = \frac{q^{\hat{+}}}{\mathbb{Q}^2} = \frac{(q\cdot n)}{\mathbb{Q}^2}, \tag{B35a}$$

$$Y = -\frac{q^2}{\mathbb{Q}^2}, \tag{B35b}$$

$$Z = -\frac{\mathbb{C}}{\mathbb{Q}^2}. \tag{B35c}$$

Thus, our result agrees with Eq. (35) derived in the main text.

Similar manipulation can be done for the longitudinal part, $\mathcal{L}_{\hat{\mu}\hat{\nu}} = \epsilon^*_{\hat{\mu}}(q,0)\epsilon_{\hat{\nu}}(q,0)$, yielding

$$\mathcal{L}_{\hat{\mu}\hat{\nu}} = \frac{(q^{\hat{+}})^2}{(q)^2\mathbb{Q}^2}\begin{pmatrix} L^2 & Lq_1 & Lq_2 & Lq_{\hat{-}} \\ Lq_1 & q_1^2 & q_1q_2 & q_{\hat{-}}q_1 \\ Lq_2 & q_1q_2 & q_2^2 & q_{\hat{-}}q_2 \\ Lq_{\hat{-}} & q_{\hat{-}}q_1 & q_{\hat{-}}q_2 & q_{\hat{-}}^2 \end{pmatrix}, \tag{B36}$$

where we introduced for convenience

$$L = q_{\hat{+}} - \frac{(q)^2}{q^{\hat{+}}}.$$

Notice that, because we are dealing with virtual photons, we have replaced M^2 by $P^{\hat{\mu}}P_{\hat{\mu}} = q^2$ in the longitudinal polarization vector given by Eq. (22c). Written in a general form, this gives Eq. (39).

APPENDIX C: PHOTON PROPAGATOR DECOMPOSITION ON THE LIGHT FRONT

Because $\mathbb{C} = 0$, there is only one pole at $\mathbf{q}_\perp^2/2q^+ - i\epsilon/2q^+$ for the first term in Eq. (42). When $q^+ > 0$, the pole is in the lower half-plane, and when $q^+ < 0$, the pole is in the upper half-plane. So, for the first term in Eq. (42), we separate the q^+ integral into two regions,

$$\int \frac{d^2\mathbf{q}_\perp}{(2\pi)^4}\left[\int_0^\infty dq^+ e^{-i(q^+x^- - \mathbf{q}^\perp\mathbf{x}^\perp)} I + \int_{-\infty}^0 dq^+ e^{-i(q^+x^- - \mathbf{q}^\perp\mathbf{x}^\perp)} I\right], \tag{C1}$$

where

$$I = \int_{-\infty}^\infty dq^- e^{-iq^-x^+}\frac{\mathcal{T}_{\mu\nu}}{2q^-q^+ - \mathbf{q}_\perp^2 + i\epsilon}. \tag{C2}$$

To evaluate I, we close the contour in the plane where the arc contribution is zero. This means we close the contour in the upper (lower) half-plane when $x^+ < 0$ ($x^+ > 0$). For the factor I in the first term of Eq. (C1), the only nonzero contribution comes from the pole that is in the lower half-plane, which is picked up when we close the contour from below ($x^+ > 0$). Similarly, for the factor I in the second term of Eq. (C1), the only nonzero contribution comes from the pole that is in the upper half-plane, which is picked up when we close the contour from above ($x^+ < 0$). Thus, Eq. (C1) becomes

$$\int \frac{d^2\mathbf{q}_\perp}{(2\pi)^4}\mathcal{T}_{\mu\nu}\left[\int_0^\infty dq^+ e^{-i(q^+x^- - \mathbf{q}^\perp\mathbf{x}^\perp)}(-2\pi i)\Theta(x^+)\frac{e^{-iHx^+}}{2q^+} + \int_{-\infty}^0 dq^+ e^{-i(q^+x^- - \mathbf{q}^\perp\mathbf{x}^\perp)}(2\pi i)\Theta(-x^+)\frac{e^{iHx^+}}{2q^+}\right], \tag{C3}$$

where $H = |\mathbf{q}_\perp^2/2q^+|$.

We now make changes of the variables $q^+ \to -q^+$ and $\mathbf{q}_\perp \to -\mathbf{q}_\perp$ in the second term that is proportional to $\Theta(-x^+)$ in order to have the limits on the q^+ integral become the same as the first term. We can then combine these two terms. This gives us

$$\begin{aligned} &i\int \frac{d^2\mathbf{q}_\perp}{(2\pi)^3}\int_0^\infty \frac{dq^+}{2q^+}\mathcal{T}_{\mu\nu}[\Theta(x^+)e^{-iHx^+}e^{-i(q^+x^- - \mathbf{q}^\perp\mathbf{x}^\perp)} \\ &\quad + \Theta(-x^+)e^{iHx^+}e^{i(q^+x^- - \mathbf{q}^\perp\mathbf{x}^\perp)}] \\ &= i\int \frac{d^2\mathbf{q}_\perp}{(2\pi)^3}\int_0^\infty \frac{dq^+}{2q^+}\mathcal{T}_{\mu\nu}[\Theta(x^+)e^{-iq_\mu x^\mu} + \Theta(-x^+)e^{iq_\mu x^\mu}]. \end{aligned} \tag{C4}$$

Since we have made the change of variables and the q^+ cannot be negative anymore, we now have $q^- = H = \mathbf{q}_\perp^2/2q^+$ in q_μ.

The second term in Eq. (42) gives straightforwardly the same result as the last term in Eq. (44), where $\mathbb{C} = 0$ (LFD). Putting everything together, we can write Eq. (42) in the LFD as

$$\begin{aligned} &i\int \frac{d^2\mathbf{q}_\perp}{(2\pi)^3}\int_0^\infty \frac{dq^+}{2q^+}\mathcal{T}_{\mu\nu}[\Theta(x^+)e^{-iq_\mu x^\mu} + \Theta(-x^+)e^{iq_\mu x^\mu}] \\ &\quad + i\delta(x^+)\int \frac{d^2\mathbf{q}_\perp}{(2\pi)^3}\int_{-\infty}^\infty dq^+ \frac{n_\mu n_\nu}{q^{+2}}e^{-i(q^+x^- + \mathbf{q}_\perp\mathbf{x}^\perp)}. \end{aligned} \tag{C5}$$

APPENDIX D: TIME-ORDERED SCATTERING AMPLITUDES FOR ϕ^3 THEORY

In ϕ^3 theory, the scattering shown in Fig. 1 involves the exchange of the scalar particle. Ignoring the inessential factors including the square of the coupling constant, we can write the time-ordered scattering amplitudes as those used in Ref. [21],

$$\mathcal{M}^{(a)} = \frac{1}{2Q^{\hat{+}}}\frac{1}{q^{\hat{+}} - Q^{\hat{+}}}, \tag{D1a}$$

$$\mathcal{M}^{(b)} = -\frac{1}{2Q^{\hat{+}}}\frac{1}{q^{\hat{+}} + Q^{\hat{+}}}, \tag{D1b}$$

where $Q^{\hat{+}}$ is defined in Eq. (71).

We use the same kinematics used for the sQED case, i.e., $\mathbf{q}_\perp = 0$. Because the kinematics is the same, the boosted q' satisfies the same equations as listed in Eq. (91). Using Eq. (6), we can also get the boosted $q'_{\hat{\mu}}$ and $q'^{\hat{\mu}}$, which can then be used to calculate the scattering amplitudes in the boosted frame.

The amplitudes are given by the functions of m_1, m_2, p, and θ. For comparison, we use the same parameter values that we used for plotting Fig. 2 in sQED, i.e., $m_1 = 1$, $m_2 = 2$, $p = 3$, and $\theta = \pi/3$. $\mathcal{M}^{(a)}$ and $\mathcal{M}^{(b)}$ with the J curve depicted by the solid red line are plotted in Fig. 4. Comparing it to Fig. 2, we see that the photon propagator modifies the profiles of the time-ordered amplitudes. Nevertheless, the J curve remains the same and is still given by Eq. (93).

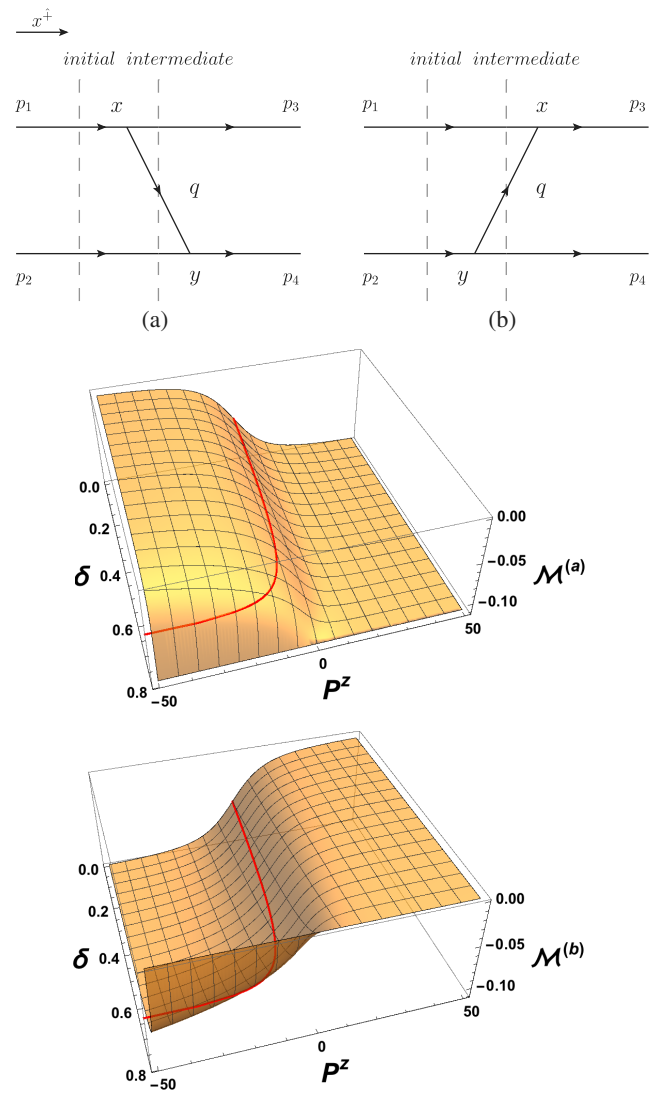

FIG. 4 (color online). Time-ordered scattering diagrams and corresponding amplitudes for the ϕ^3 theory.

APPENDIX E: TIME-ORDERED ANNIHILATION AMPLITUDES IN sQED

For the sQED annihilation process analogous to $e^+e^- \to \mu^+\mu^-$ in QED, we can still use Fig. 1 for the kinematics. Three time-ordered diagrams corresponding to the lowest-order amplitudes are shown in Fig. 5. Here, the amplitude of Eq. (70) changes to

$$\begin{aligned} i\mathcal{M} &= \sum_{j=a,b,c} i\mathcal{M}^{(j)} \\ &= (-ie)^2 \sum_{j=a,b,c} (p_3^{\hat{\mu}} - p_4^{\hat{\mu}})\Sigma^{(j)}_{\hat{\mu}\hat{\nu}}(p_1^{\hat{\nu}} - p_2^{\hat{\nu}}). \end{aligned} \tag{E1}$$

The time-ordered amplitudes are given by

$$\mathcal{M}^{(a)} = -(-ie)^2 \frac{[p_{34}\cdot p_{12} + p_{34}^{\hat{+}} p_{12}^{\hat{+}} q^2/(Q^{\hat{+}})^2]\mathbb{C}}{2Q^{\hat{+}}(q^{\hat{+}} - Q^{\hat{+}})}, \tag{E2a}$$

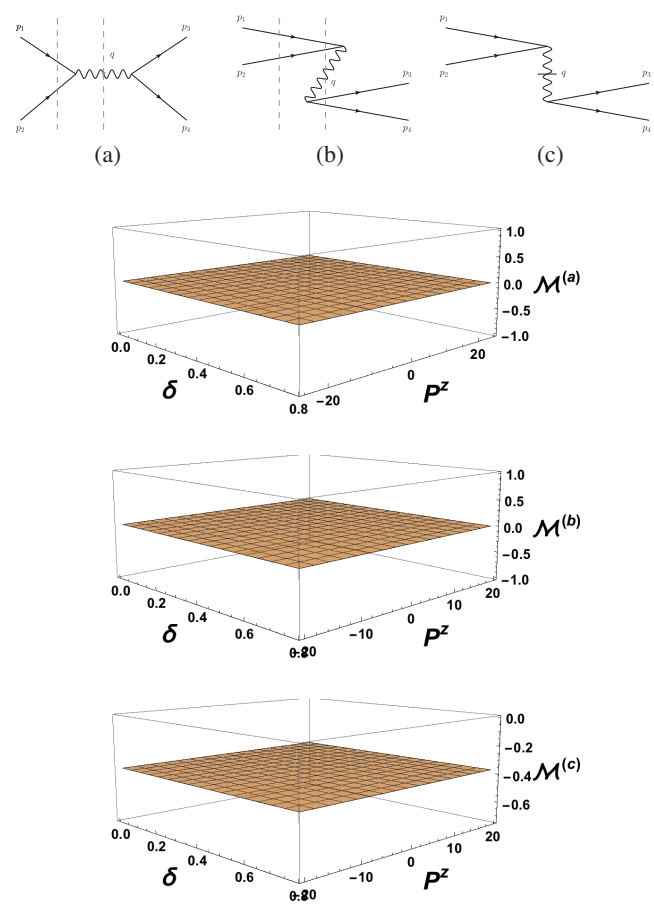

FIG. 5 (color online). Time-ordered annihilation diagrams and their amplitudes for sQED.

$$\mathcal{M}^{(b)} = (-ie)^2 \frac{[p_{34}\cdot p_{12} + p_{34}^{\hat{+}} p_{12}^{\hat{+}} q^2/Q^{\hat{+}})^2]\mathbb{C}}{2Q^{\hat{+}}(q^{\hat{+}} + Q^{\hat{+}})}, \tag{E2b}$$

$$\mathcal{M}^{(c)} = (-ie)^2 \frac{p_{34}^{\hat{+}} p_{12}^{\hat{+}}}{(Q^{\hat{+}})^2}, \tag{E2c}$$

where

$$p_{34} = p_3 - p_4, \tag{E3a}$$

$$p_{12} = p_1 - p_2, \tag{E3b}$$

and $q = p_1 + p_2$. We use the same kinematics (CMF) as before so that p_i's are given by

$$p_1 = (\epsilon, 0, 0, p), \tag{E4a}$$

$$p_2 = (\epsilon, 0, 0, -p), \tag{E4b}$$

$$p_3 = (\epsilon, p_f \sin\theta, 0, p_f \cos\theta), \tag{E4c}$$

$$p_4 = (\epsilon, -p_f \sin\theta, 0, -p_f \cos\theta). \tag{E4d}$$

Since we are considering the annihilation process, the initial particles 1 and 2 should have the same mass, and the final particles 3 and 4 should have the same mass. So, we set $m_1 = m_2 = m$ and $m_3 = m_4 = m_f$. Because of the energy conservation, all four particles should have the same energy in the CMF, and p and p_f are therefore related by $p_f = \sqrt{q^2 + m^2 - m_f^2}$. The boosted p'_i's still follow Eq. (90). Thus, q' in the annihilation process is rather simple:

$$q'^x = p'^x_1 + p'^x_2 = 0, \tag{E5a}$$

$$q'^y = p'^y_1 + p'^y_2 = 0, \tag{E5b}$$

$$q'^z = p'^z_1 + p'^z_2 = P^z, \tag{E5c}$$

$$q'^0 = p'^0_1 + p'^0_2 = E. \tag{E5d}$$

Applying Eq. (90) to Eqs. (E3a) and (E3b) with p_i given by Eq. (E4), we find that

$$p'_{34}\cdot p'_{12} = -4p\sqrt{m^2 - m_f^2 + p^2}\cos\theta, \tag{E6a}$$

$$q'^2 \frac{p'^{\hat{+}}_{34} p'^{\hat{+}}_{12}}{(Q'^{\hat{+}})^2} = 4p\sqrt{m^2 - m_f^2 + p^2}\cos\theta. \tag{E6b}$$

So the numerators in Eqs. (E2a) and (E2b) are zero, regardless of the frame or the interpolation angle δ. Therefore, $\mathcal{M}^{(a)} = \mathcal{M}^{(b)} = 0$, and the only nonzero contribution comes from the instantaneous interaction. One can verify that indeed the covariant total amplitude is the same as $\mathcal{M}^{(c)}$,

$$\mathcal{M}^{(c)} = \mathcal{M} = -\frac{p_{34}\cdot p_{12}}{q^2} = -\frac{p\sqrt{m^2 - m_f^2 + p^2}\cos\theta}{m^2 + p^2}, \tag{E7}$$

where the coupling constant e is taken as 1. We can see that this result is also independent of the frame and interpolation angle, just as expected.

In Fig. 5, we again use the same parameter values as before: $m = 1$, $m_f = 2$, $p = 3$, and $\theta = \pi/3$. The corresponding time-ordered amplitudes shown here are all flat planes.

[1] P. Dirac, Rev. Mod. Phys. **21**, 392 (1949).
[2] S. Fubini, A. J. Hanson, and R. Jackiw, Phys. Rev. D **7**, 1732 (1973).
[3] L. Y. Glozman, W. Plessas, K. Varga, and R. F. Wagenbrunn, Phys. Rev. D **58**, 094030 (1998); R. Wagenbrunn, S. Boffi, W. Klink, W. Plessas, and M. Radici, Phys. Lett. B **511**, 33 (2001); T. Melde, K. Berger, L. Canton, W. Plessas, and R. Wagenbrunn, Phys. Rev. D **76**, 074020 (2007).
[4] P. J. Steinhardt, Ann. Phys. (N.Y.) **128**, 425 (1980).
[5] S. Weinberg, Phys. Rev. **150**, 1313 (1966); J. Jersák and J. Stern, Nucl. Phys. **B7**, 413 (1968).
[6] J. Bjorken, Phys. Rev. **179**, 1547 (1969); S. D. Drell, D. Levy, and T. M. Yan, Phys. Rev. **187**, 2159 (1969).
[7] H. C. Pauli and S. Brodsky, Phys. Rev. D **32**, 1993 (1985); S. J. Brodsky and H. C. Pauli, *Recent Aspects of Quantum Fields*, Lecture Notes in Physics, edited by H. Mitter and H. Gausterer (Springer, Berlin, 1991), Vol. 396, p. 51.
[8] R. Perry, A. Harindranath, and K. Wilson, Phys. Rev. Lett. **65**, 2959 (1990); R. Perry and A. Harindranath, Phys. Rev. D **43**, 4051 (1991); D. Mustaki, S. Pinsky, J. Shigemitsu, and K. Wilson, Phys. Rev. D **43**, 3411 (1991).
[9] S. Brodsky, J. Hiller, and G. McCartor, Phys. Rev. D **58**, 025005 (1998); J. R. Hiller, arXiv:hep-ph/9807245.
[10] D. G. Robertson and G. McCartor, Z. Phys. C **53**, 661 (1992); G. McCartor and D. G. Robertson, Z. Phys. C **53**, 679 (1992).

[11] S. Brodsky, H. C. Pauli, and S. Pinsky, Phys. Rep. **301**, 299 (1998).
[12] L. Susskind and M. Burkardt, *Proceedings of the 4th International Workshop on Light-Front Quantization and Nonperturbative Dynamics, Polana Zgorzelisko, Poland, 1994*, edited by S. D. Glazek (World Scientific, Singapore, 1995), p. 5; K. G. Wilson and D. G. Robertson, *Proceedings of the 4th International Workshop on Light-Front Quantization and Nonperturbative Dynamics, Polana Zgorzelisko, Poland, 1994*, edited by S. D. Glazek (World Scientific, Singapore, 1995), p. 15.
[13] C.-R. Ji and Y. Surya, Phys. Rev. D **46**, 3565 (1992).
[14] K. Hornbostel, Phys. Rev. D **45**, 3781 (1992).
[15] C.-R. Ji and S.-J. Rey, Phys. Rev. D **53**, 5815 (1996).
[16] T. Chen, Phys. Rev. D **3**, 1989 (1971).
[17] E. Elizalde and J. Gomis, Il Nuovo Cimento A Series 11 **35**, 367 (1976); Nucl. Phys. **B122**, 535 (1977); J. Math. Phys. (N.Y.) **19**, 1790 (1978).
[18] Y. Frishman, C. Sachrajda, H. Abarbanel, and R. Blankenbecler, Phys. Rev. D **15**, 2275 (1977).
[19] M. Sawicki, Phys. Rev. D **44**, 433 (1991).
[20] C.-R. Ji and C. Mitchell, Phys. Rev. D **64**, 085013 (2001).
[21] C.-R. Ji and A. T. Suzuki, Phys. Rev. D **87**, 065015 (2013).
[22] G. P. Lepage and S. J. Brodsky, Phys. Rev. D **22**, 2157 (1980).
[23] A. Bassetto, M. Dalbosco, and R. Soldati, Phys. Rev. D **36**, 3138 (1987); A. Bassetto, G. Heinrich, Z. Kunszt, and W. Vogelsang, Phys. Rev. D **58**, 094020 (1998).
[24] G. Leibbrandt, Rev. Mod. Phys. **59**, 1067 (1987); Nucl. Phys. **B310**, 405 (1988); G. Leibbrandt and J. Williams, Nucl. Phys. **B566**, 373 (2000).
[25] G. Leibbrandt, Phys. Rev. D **29**, 1699 (1984).
[26] P. Srivastava and S. Brodsky, Phys. Rev. D **64**, 045006 (2001).
[27] A. T. Suzuki and J. H. O. Sales, Nucl. Phys. **A725**, 139 (2003); Mod. Phys. Lett. A **19**, 1925 (2004); **19**, 2831 (2004); A. Misra and S. Warawdekar, Phys. Rev. D **71**, 125011 (2005).
[28] M. Jacob and G. Wick, Ann. Phys. (N.Y.) **7**, 404 (1959).
[29] J. J. Sakurai, *Modern Quantum Mechanics*, 2nd ed., (Pearson, San Francisco, CA, USA, 2011), p. 175.
[30] D. Soper, SLAC Report No. 137, 1971.
[31] L. H. Ryder, *Quantum Field Theory*, 2nd ed. (Cambridge University Press, Cambridge, England, 1996), p. 141.
[32] J. Kogut and D. Soper, Phys. Rev. D **1**, 2901 (1970).